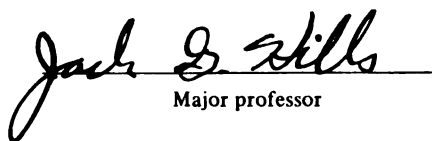


This is to certify that the
thesis entitled
COMPUTER SIMULATIONS OF
GRAVITATIONAL ENCOUNTERS BETWEEN
PAIRS OF BINARY STAR SYSTEMS
presented by
James Brian Hoffer

has been accepted towards fulfillment
of the requirements for
Ph.D. degree in Physics


Major professor

Date March 1, 1983



RETURNING MATERIALS:
Place in book drop to
remove this checkout from
your record. **FINES** will
be charged if book is
returned after the date
stamped below.

NO FINE CHARGES

ROOM USE ONLY

COMPUTER SIMULATIONS OF
GRAVITATIONAL ENCOUNTERS BETWEEN
PAIRS OF BINARY STAR SYSTEMS

by

James Brian Hoffer

A DISSERTATION

Submitted to
Michigan State University
in partial fulfillment of the requirements
for the degree of

Doctor of Philosophy

Department of Physics and Astronomy

1983

157-4646

ABSTRACT
COMPUTER SIMULATIONS OF
GRAVITATIONAL ENCOUNTERS BETWEEN
PAIRS OF BINARY STAR SYSTEMS

by

James B. Hoffer

Encounters (collisions) between pairs of binary stars were computer-simulated. The 41,564 collisions were divided into five mass families and all binaries initially had circular orbits.

The exchanged energy cross-section for collisions between two binaries composed of identical mass stars was found to be roughly 2-3 times that for a single star colliding with a binary having components with masses equal to that of the single star. Other results cannot be stated so easily, but the energy released by hard binary collisions appears to be significant.

A surprising result is that roughly 40% of the binary-binary collisions in a globular cluster core precipitate a physical collision between two stars, possibly leading to their coalescence.

To increase the speed of the integrator, a technique was developed whereby each tightly bound binary is treated as a

single star until it is intruded upon by another member of the system. Experiments have shown that this technique can decrease the required integration time by an order of magnitude without affecting the statistics of the collisions appreciably.

Each collision was allowed a certain number of integration steps (50,000-100,000) to reach a final, stable configuration consisting of only single stars and binaries. If such a configuration could not be reached within the prescribed limits, an attempt was made to find the (intermediate) results and the collision was aborted. These results were not used in computing the statistics of that set of collisions.

to my Florina

ACKNOWLEDGMENTS

I would first like to express my thanks to Dr. Jack G. Hills, my advisor throughout this project. He introduced me to the field of theoretical dynamics and suggested this dissertation project. He showed me that one of my favorite topics, orbital motion, is still an area of active and interesting research.

I am thankful for the support of Dr. Robert F. Stein in the form of computer time both for performing a large fraction of these collisions and for producing this dissertation in the present physical form with the aid of his text processor.

I am very appreciative of the support given to me by the Los Alamos National Laboratory through computer time. It was at LANL that I performed virtually all of the hard collisions and many of the soft collisions in this dissertation.

The Departments of Physics, Astronomy, and Physics and Astronomy graciously provided support in the form of graduate assistantships throughout my tenure at Michigan State University. I thank the Department of Physics for its support in the form of many hours of computer time also.

I am appreciative of the support I have received from my family and friends at Michigan State University and elsewhere.

Most importantly, for her enduring support throughout, I thank Florina, my fiancée, to whom this dissertation is lovingly dedicated.

TABLE OF CONTENTS

	Page
LIST OF TABLES	vii
LIST OF FIGURES	viii
 CHAPTER	
1. INTRODUCTION	1
1.1. Binary Systems in Star Clusters	1
1.2. Historical	3
1.3. Research Purpose	4
2. COMPUTATIONAL TECHNIQUES	7
2.1. Introduction	7
2.2. The Regularization Technique	8
2.3. The Reduction of Close Binaries	14
2.4. Kepler's Equation	17
2.5. Kinetic Energy at Infinite Separation	21
3. THE PROGRAM	24
3.1. Introduction	24
3.2. Organization of Collisions	24
3.3. Initializing a Collisions	25
3.4. The Integration Routine	28
3.5. The Beginning and Ending of a Collision	30
4. ANALYSIS OF RESULTS	34
4.1. Introduction	34
4.2. The Exchange of Energy	35
4.2.1. Introduction	35
4.2.2. The Exchange of Energy at Zero Impact Parameter	36
4.2.3. The Exchange of Energy Versus Impact Parameter	45
4.2.4. The Exchanged Energy Cross-Section	48
4.3. The Final Configuration	52
4.4. The Average Eccentricity of the Surviving Binaries	59

4.5.	The Distance of Closest Approach	61
5.	CONCLUSIONS	65
5.1.	Comparison of Present with Previous Results	65
5.2.	Future Investigations of Binary-Binary Collisions	68
	LIST OF REFERENCES	71
	APPENDICES	
A.	THE DATA	73
B.	GLOSSARY OF TERMS	86

LIST OF TABLES

TABLE		Page
1.	The results of least squares fits of the data to equation (4.6).	44
2.	A summary of least squares fits of the data to equation (4.12).	47
3.	A summary of least squares fits of the data in families A and B to equation (4.13).	48
4.	Conversion factors from the present experiment to HF's experiment.	66
5.	A summary of the results of the collisions.	74

LIST OF FIGURES

FIGURE		Page
1.	A typical run-summary for a group of collisions.	26
2.	Two samples of collision results.	27
3.	Plots of ξ and $\log(\xi\alpha^{1/2})$ versus $\log\alpha$ for family A.	37
4.	Plots of ξ and $\log(\xi\alpha^{1/2})$ versus $\log\alpha$ for family B.	38
5.	Plots of ξ and $\log(\xi\alpha^{1/2})$ versus $\log\alpha$ for family C.	39
6.	Plots of ξ and $\log(\xi\alpha^{1/2})$ versus $\log\alpha$ for family D.	40
7.	Plots of ξ and $\log(\xi\alpha^{1/2})$ versus $\log\alpha$ for family E.	41
8.	Plots of $\log(\sigma_E)$ versus $\log\alpha$ using equation (4.19) and the data from Tables 1 and 3.	51
9.	Probability of no change versus $\log\alpha$	53
10.	Probability of exchange versus $\log\alpha$	55
11.	Probability of a single binary versus $\log\alpha$	56
12.	Probability of dissociation versus $\log\alpha$	58
13.	Average eccentricity versus $\log\alpha$	60
14.	Logarithm of the average distance of closest approach versus $\log\alpha$	62
15.	The orientational orbital elements.	88
16.	The orbital plane.	89

CHAPTER 1
INTRODUCTION

1.1. Binary Systems in Star Clusters

In 1972 Aarseth and Hills performed a computer experiment attempting to rectify the disagreement between theory and observation regarding open clusters. Star-formation theory predicts that, if all the stars in a cluster are formed from the same gas cloud, there should be some clumpiness in their spatial distribution. This occurs because, as the cloud contracts under the action of its self-gravity, its density increases causing the gravitational Jeans length to decrease. The cloud then breaks up into subclouds. Each subcloud then contracts to the point where it breaks up into sub-subclouds. This division process continues until a typical subcloud has dimensions appropriate for star-formation to occur. Thus the initial cloud forms a hierarchy of subclouds. According to this model, we should expect the density of a cluster to be non-uniform; a certain clumpiness in the spatial distribution of the stars should be observed. This clumpiness is not observed in mature open clusters, however, it is found in molecular-hydrogen proto-clusters observed by radio telescope (Larson 1981).

The Aarseth-Hills computer model began with a cluster of stars having a clumpy appearance. The stars were arranged so that a hierarchy of subclustering was present. The cluster was then allowed to develop according to the law of classical gravitation. In a single collapse time, it evolved a fairly homogeneous form, but almost more interesting was that the cluster was forming binary stars by three-star encounters. By the termination of the experiment at 4.2 collapse times, the cluster was composed of 6.2% binaries. After subtraction of the number of stars that had escaped from the cluster, this becomes 10.8%. While this is not an incredibly large percentage, these binaries had acquired more than 90% of the total binding energy of the cluster. Clearly the dynamical evolution of this small percentage of binary stars as mediated through collisions becomes important in determining the dynamical evolution of a cluster. As the number of binaries increases, the frequency of collisions involving them also increases.

Another demonstration of the importance of binary stars in the dynamical evolution of a star system was given by Spitzer and Mathieu (1980) when they modeled the dynamics of some globular clusters. In their models, they attempted to account for the effects of collisions between single and binary stars as well as between two binaries. The single-binary collisions were fairly well understood at the time, but binary-binary collisions were not. Their treatment of binary-binary collisions as successive single-binary

collisions seems less than adequate, but better than ignoring them altogether. Their globular cluster models initially contained 50% and 20% of the total mass in binaries. After $1600 \tau_{rh}$ (τ_{rh} is the relaxation time of the stars in a sphere about the center of mass of the cluster and enclosing half of the mass), the central region of each cluster contained 90% and 80% of its mass in binaries. At such high concentrations of binaries, interactions involving them become extremely important. Clearly these interactions (collisions) must be understood if a correct model of the dynamical evolution of the core of a globular cluster is to be obtained.

1.2. Historical

After the Aarseth-Hills investigation of the dynamical evolution of an open cluster, investigations were begun with the goal of obtaining an understanding of collisions involving binary systems. Probably because they are the simplest as well as the most common at low binary densities, collisions between single stars and binaries were investigated first. This investigation was launched from two fronts.

Heggie attacked the problem from a purely theoretical direction. His analytical treatment of the statistics of these collisions (Heggie 1975) is quite complete and gives a formalism into which experimental results can be cast. To verify the accuracy of several equations, he performed a

rather incomplete set of collisions on a computer.

Hills took the computer-experimental approach (Hills 1975). With Fullerton (Hills and Fullerton 1980; Fullerton and Hills 1982), he has completed, analyzed, and published the results of some 65,096 computer collisions between single stars and binaries. While this treatment is complete as far as it goes, nearly all of these collisions were performed with the initial eccentricity of the binary being zero. Whether these statistics are representative of elliptical orbit statistics remains to be seen.

Valtonen also has performed simulations of interactions between single and binary stars (Valtonen 1975). However, his interest was the decay of quasi-stable three-body systems and is not directly applicable here.

All of the above work concerns the interaction of single stars with binaries. Presently only one experiment has been performed involving two binaries. Saslaw, Valtonen, and Aarseth (1974) have performed 200 simulations of the decay of quasi-stable two-binary systems. No collisions between two binary systems have been performed.

1.3 Research Purpose

The purpose of this investigation is to examine collisions between two binary star systems. These collisions are assumed to be completely Newtonian-gravitational in nature as well as independent of the structure and evolution of the stellar components. The gravitational

interaction among four point-masses is our only concern. 41,564 of these collisions were performed with the aid of several computers. The salient features of the computer program as well as the reduction of the data will be presented in this dissertation.

The collisions are divided into five families, A-E, according to the masses of the components. Only the relative masses will be given since the equations of motion for the system are linear in the masses and, hence, can experience a mass scale change resulting only in a change of scale of the physical time. The families and their associated masses are:

A	(1-1)-(1-1)
B	(3-3)-(1-1)
C	(1-3)-(1-3)
D	(10-10)-(1-1)
E	(1-10)-(1-10).

The notation (a-b)-(c-d) signifies that initially a star with mass a is part of a binary with another star of with mass b. This is similarly true for stars c and d. The two binaries are then caused to collide. Each family contains groups of collisions with usually 200 collisions in each group. Each group is specified by: the initial ratio of the kinetic energy of the binaries at infinite separation to the energy required for complete dissociation of the system (α), the ratio of the binding energies of the binaries (β), the

impact parameter (p) in units of the initial separation of binary ($a-b$), and the initial eccentricities of the binaries which are zero for all cases considered. The remaining quantities are randomly sampled by a Monte Carlo technique and will be discussed later in this dissertation.

CHAPTER 2

COMPUTATIONAL TECHNIQUES

2.1. Introduction

It is well known that the equations of motion for the gravitational three-body problem (TBP) have no analytic solution. Any analytic approximations break down nearly completely during very close approaches among the members of such a system during which the equations of motion become mathematically poorly-behaved. The gravitational four-body problem (FBP) suffers from the same difficulties as the TBP, but they are even more severe because of the increase in the likelihood of very close approaches. However, this difficulty can be significantly reduced through the process of regularization (simplification of the equations of motion by reparameterization) to be described in some detail later. Because the FBP is not analytically solvable, solutions to its equations of motion must be found by some approximation technique. In the present investigation, the solutions will be found numerically with the aid of a computer. In addition to integration and roundoff error, the length of time the computer requires to find the final, stable configuration of the entire system must be considered. In particular, the formation of quasi-stable configurations is

of interest. A common occurrence at low collision energies is the formation of a tightly bound binary as a component of a loosely bound binary, i.e. a quasi-stable trinary. While this configuration is not generally mathematically stable, an inordinately large quantity of computer time is usually needed to test its long-term stability unless some special technique is used to increase the integration speed.

The two problems described above constitute the major problems encountered when integrating the equations of motion for the FBP. The techniques developed to reduce these difficulties introduced two fairly minor, additional problems. These techniques required that Kepler's Equation be solved more than 10^5 times. The large number of solutions needed requires that the method devised to find the solution be extremely reliable, sacrificing speed if need be. The other additional difficulty occurs at the end of a collision where the kinetic energies of all unbound bodies must be found as the separations become infinite. Since the FBP is not analytically solvable, approximations to the problem must be made if these quantities are to be found while the separations are still finite.

2.2. The Regularization Technique

In integrating the equations of motion for the FBP, one finds that the separations between the masses can vary by as much as several orders of magnitude. In order to maintain accuracy, one would like to decrease the increment of the

independent variable (time) when the group is compact while increasing it when the group is dispersed. This can be accomplished either explicitly or by the more elegant technique of regularization which transforms the time coordinate so as to remove the singularity produced when two objects make an exceptionally close approach to each other. Such close approaches may cause a large error in the total energy of the system because of the large velocities involved and because of the finite precision afforded by computers.

The regularization method employed for this calculation is the technique of multi-particle, quasi-regularization in time developed by Heggie (1972). The equations of motion are regularized by a replacement of the physical time with a regularized time. These are related by

$$d\tau = h(x_{ij}, \dot{x}_{ij}) dt \quad (2.1)$$

where dt is the increment of the physical time, $d\tau$ is the increment of the regularized time, x_{ij} is the j -th (cartesian) component of the i -th mass, and h is called the regularizing function. The dot indicates the total physical time derivative of the quantity under it.

The equations of motion can be written very simply as

$$\ddot{x}_{ij} = a_{ij} \quad (2.2)$$

where a_{ij} is the j -th (cartesian) component of the acceleration (force per unit mass) of the i -th mass. Now, by the

chain rule of differential calculus, we have the operational relation

$$d/dt = d\tau/dt d/d\tau \quad (2.3)$$

or, after applying equation (2.1), we can write

$$d/dt = h(x_{ij}, \dot{x}_{ij}) d/d\tau. \quad (2.4)$$

If a primed quantity denotes the total regularized time derivative of the quantity, then we have from equation (2.4),

$$\dot{x}_{ij} = h(x_{ij}, \dot{x}_{ij}) x_{ij}'. \quad (2.5)$$

Total differentiation of equation (2.5) with respect to the physical time t gives

$$\ddot{x}_{ij} = \dot{h}(x_{ij}, \dot{x}_{ij}) x_{ij}' + h(x_{ij}, \dot{x}_{ij}) \dot{x}_{ij}'. \quad (2.6)$$

After applying equation (2.4) to equation (2.6), we obtain

$$\begin{aligned} \ddot{x}_{ij} &= h(x_{ij}, \dot{x}_{ij}) h'(x_{ij}, \dot{x}_{ij}) x_{ij}' \\ &+ h^2(x_{ij}, \dot{x}_{ij}) x_{ij}''. \end{aligned} \quad (2.7)$$

By solving equation (2.7) for x_{ij}'' , we obtain a new set of differential equations in x_{ij} :

$$\begin{aligned} x_{ij}'' &= h^{-2}(x_{ij}, \dot{x}_{ij}) a_{ij} \\ &- h'(x_{ij}, \dot{x}_{ij}) x_{ij}' / h(x_{ij}, \dot{x}_{ij}) \end{aligned} \quad (2.8)$$

where a_{ij} has been written instead of \ddot{x}_{ij} according to

equation (2.2).

Even though equation (2.8) provides a recipe for finding x_{ij} , it is more convenient to rewrite it utilizing a regularizing function that contains the dynamical quantities and their regularized time derivatives rather than keeping their physical time derivatives. We define a new regularizing function $g(x_{ij}, x_{ij}')$ such that

$$g(x_{ij}, x_{ij}') = h(x_{ij}, \dot{x}_{ij}). \quad (2.9)$$

This gives a new, consistent set of equations of motion.

$$\begin{aligned} x_{ij}'' &= g^{-2}(x_{ij}, x_{ij}')a_{ij} \\ &- g'(x_{ij}, x_{ij}')x_{ij}'/g(x_{ij}, x_{ij}') \end{aligned} \quad (2.10)$$

An appropriate $g(x_{ij}, x_{ij}')$ will now be chosen so that equation (2.10) is well behaved as the separations of the component masses vanish.

If equation (2.10) is to be convergent as the separations vanish, then the conditions

$$\lim_{R \rightarrow 0} |g^{-2}(x_{ij}, x_{ij}')a_{ij}| < \infty \quad (2.11)$$

and

$$\lim_{R \rightarrow 0} |g'(x_{ij}, x_{ij}')x_{ij}'/g(x_{ij}, x_{ij}')| < \infty \quad (2.12)$$

must be satisfied. R is the minimum of the six separations of each body from each other body. Relation (2.11) can be

satisfied if $g(x_{ij}, x_{ij}')$ diverges at least as fast as R vanishes since the dominating term in a_{ij} is proportional to $1/R^2$. A function satisfying this condition is the total potential energy of the system. For the FBP this is

$$U = - \sum_{i=2}^4 \sum_{k=1}^{i-1} Gm_i m_k / r_{ik} \quad (2.13)$$

where r_{ik} is the separation of the masses m_i and m_k .

To find whether relation (2.12) is satisfied, we must differentiate equation (2.13) with respect to the regularized time.

$$g'(x_{ij}, x_{ij}') = dU/d\tau = - \sum_{i=2}^4 \sum_{k=1}^{i-1} (Gm_i m_k / r_{ik}^3) \dot{r}_{ik} \cdot \dot{r}_{ik}'. \quad (2.14)$$

We now see that the left side of relation (2.12) goes as x'^2/R for very close approaches which, by equation (2.5), we can rewrite as $\dot{x}^2 \times R$. Conservation of energy tells us that this quantity converges as R vanishes (it varies linearly with R for the two-body case with zero angular momentum). The use of the potential energy for the regularizing function satisfies the necessary conditions and works well in practice, so we will use it.

In summary, the set of equations we wish to solve is

$$\begin{aligned} x_{ij}'' &= g^{-2}(x_{ij}, x_{ij}') a_{ij} \\ &- g'(x_{ij}, x_{ij}') x_{ij}' / g(x_{ij}, x_{ij}') \end{aligned} \quad (2.15)$$

with

$$g(x_{ij}, x'_{ij}) = U = - \sum_{i=2}^4 \sum_{k=1}^{i-1} G_{im_k} / r_{ik} \quad (2.16)$$

and

$$a_{ij} = - \sum_{k=1}^4 \overset{\prime}{G}_{mk} / r_{ik}^3 \overset{\prime}{r}_{ik}. \quad (2.17)$$

The primed summation indicates that the sum is over all k except for $k=i$. Notice that this set of equations contains only the dynamical variables x and x' ; the physical time has been eliminated. When integrating the equations of motion, we need not concern ourselves with the physical time. Should it be required, we can compute it by integrating equation (2.1) in the form

$$dt = d\tau / g(x_{ij}, x_{ij}') \quad (2.18)$$

giving

$$\Delta t = \int_{\tau_0}^{\tau_1} d\tau / g(x_{ij}, x_{ij}') \quad (2.19)$$

as the physical time interval corresponding to the regularized time interval $\tau_1 - \tau_0$.

2.3. The Reduction of Close Binaries

When α is less than three, the formation of quasi-stable configurations such as trinarities and two mutually bound binaries becomes common. Each of these may persist for a very long time until it evolves into a stable configuration composed of a combination of single stars and binaries. To aid the computer in solving these cases in a reasonable and affordable amount of time, we can often treat each tightly bound binary system as a single star.

Consider a binary in the presence of a single star. The binary has components with masses m_a and m_b and orbital semi-major axis a . The single star has mass m_i and is a distance R_i from the center of mass of the binary. The gravitational force between the two members of the binary is

$$F_b = Gm_a m_b / a^2, \quad (2.20)$$

with the stars treated as point masses. The tidal force on the binary due to the field star is

$$F_{ti} = 2G(m_a + m_b)m_i a / R_i^3. \quad (2.21)$$

It tends to dissociate the binary. We can define a measure of the total tidal force due to this and all other field stars in the system to be

$$F_t = \left(\sum_{i=1}^N F_{ti}^2 \right)^{1/2}. \quad (2.22)$$

We will call the ratio of these two forces Q :

$$Q = F_b/F_t. \quad (2.23)$$

When Q is large, the disruptive efficiency of the field stars is small. When Q equals or exceeds some value (10^5 was used in practice), the perturbative effect of the field stars is considered negligible and the binary is treated as a single star until Q becomes small enough so that perturbative effects again become important. This replacement effectively eliminates a large term from the potential energy (the regularizing function), which increases the regularized time step and decreases the real computer time required to integrate the equations of motion.

The process of replacing a tightly bound binary by a single star will be called "reduction" while the inverse process will be "resolution." The reduction of a binary is accomplished by a standard procedure: the coordinates of the binary components are first transformed into the binary center-of-mass coordinate system so the orbital elements can be found. The five classical orbital elements, the semi-major axis, the eccentricity, the inclination, the longitude of the ascending node, and the argument of periastron passage are then found. A sixth quantity, the true anomaly, giving the phase of the orbit relative to periastron (closest approach in orbit), is also calculated. (For definitions of these quantities, see Appendix B.) After saving these six quantities along with the physical time, we

replace the binary by a single star with a mass equal to the sum of the masses of the binary components and coordinates (both position and velocity) described by the motion of the binary center-of-mass. The integration routine then continues with one fewer star and the absence of a large, real time-consuming term in the regularizing function.

When a reduced binary system is perturbed strongly by another star or by a group of stars, it is resolved into its original components through a knowledge of its five orbital elements, the time, the true anomaly when reduction occurred, and the new time. Kepler's Equation is used to relate these last three quantities to the new true anomaly.

It is worthwhile to note the magnitude of the contribution to the random energy error introduced by the reduction-resolution process. If a binary having components with masses m_a and m_b and semi-major axis a is perturbed by a star with mass m separated from the binary center of mass by a distance R , the random energy error introduced is of order (Hoffer 1982)

$$\delta E/E = 0.25 (a/R)^2 = [m_a m_b / 16Q(m_a + m_b)m]^{2/3}. \quad (2.24)$$

If $m_a = m_b = m$ and $Q = 10^5$, $\delta E/E = 4.6 \times 10^{-5}$. The maximum allowed relative energy error is 0.01 and this is well within that limit. In practice, the energy error was computed by actually resolving any reduced binaries and computing the energy associated with their components. The median relative energy error was approximately 10^{-4} . This is

consistent with the median error obtained in previous similar experiments by Hills (1975).

2.4. Kepler's Equation

When a reduced binary is resolved, the new true anomaly must be related to the new time, the old true anomaly, and the old time. The recipe to do this involves Kepler's Equation (Marion Chapter 8):

$$2\pi(t-t_0)/\tau = \psi - \psi_0 - e\sin\psi + e\sin\psi_0, \quad (2.25)$$

where t is the new physical time, t_0 is the old physical time, τ is the orbital period, ψ is the new eccentric anomaly, ψ_0 is the old eccentric anomaly, and e is the eccentricity of the orbital ellipse. Once ψ is obtained, the true anomaly θ can be found through the relation

$$\tan(\theta/2) = [(1+e)/(1-e)]^{1/2} \tan(\psi/2). \quad (2.26)$$

(θ and ψ are defined in Appendix B.) As long as $e < 1$, no problems arise with equation (2.26). Notice that if the tangent function is defined to exist on the half-open interval $[-\pi/2, \pi/2)$ radians, a unique θ exists for each ψ in the interval $[-\pi, \pi)$.

Kepler's Equation must be solved numerically since all attempts at analytic solution have failed (Moulton p. 162f). Since we must extract a solution several thousand times in this experiment, the most important feature of the method developed must be its consistency. We would rather use a

fairly slow method which always converges on the solution than a fast one that works only 99% of the time. For the method to be usable, it should not fail more often than once in 10^4 attempts. A higher failure rate than this would cause an unacceptable program failure rate.

In this experiment, a hybrid method was used. This hybrid consists of two parts: the first part is used to find an approximate solution and the second part uses the approximate solution to find a solution to within an accuracy of one part in 10^{-10} .

The first part of the hybrid method is the technique of successive substitution. To utilize it, we must arrange Kepler's Equation so it has the form

$$\psi = f(\psi). \quad (2.27)$$

We then substitute an approximate solution into the right side of equation (2.27) and compute a better approximation to the solution. We can write this process in iterative notation as

$$\psi_{i+1} = f(\psi_i). \quad (2.28)$$

If we call the exact solution to equation (2.27) ψ_* , then the error in successive approximations to ψ_* is (Hildebrand p. 567f)

$$\psi_* - \psi_i \approx [f'(\psi_*)]^i. \quad (2.29)$$

For convergence $|f'(\psi_*)| < 1$. Clearly the choice of $f(\psi)$ in

equation (2.27) must be made judiciously if the process is to converge upon the solution. We will choose

$$f(\psi) = \psi_0 - e \sin \psi_0 + e \sin \psi + 2\pi(t-t_0)/\tau. \quad (2.30)$$

The only other choice is to solve for ψ in the sine term, but consideration of computing the inverse sine at each iteration as well as the ambiguity in to quadrant of ψ discourages us from choosing $f(\psi)$ to be this.

The derivative of our chosen $f(\psi)$ is

$$f'(\psi) = e \cos \psi. \quad (2.31)$$

For bound orbits $|f'(\psi)| < 1$ so apparently we have made a good choice for $f(\psi)$.

This successive substitution technique was initialized with $\psi_0=1$. Five iterations were then performed resulting in a reasonable approximation to the solution of Kepler's Equation.

After obtaining a reasonable approximation to ψ_* through the method described above, we used the Newton-Raphson iterative technique to bring the error in the solution to within 10^{-10} . Even though this technique was developed by Newton expressly for the purpose of solving Kepler's Equation, unless the seed is reasonably near the exact solution, the Newton-Raphson technique may not converge. The successive substitution technique is simply a way of obtaining such a seed.

The Newton-Raphson technique is iterative in nature and may be summarized by the equation

$$\psi_{i+1} = \psi_i - f(\psi_i)/f'(\psi_i) \quad (2.32)$$

where, for the exact solution ψ_* ,

$$f(\psi_*) = 0. \quad (2.33)$$

For Kepler's Equation we choose

$$f(\psi) = \psi - \psi_0 - e \sin \psi + e \sin \psi_0 - 2\pi(t-t_0)/\tau \quad (2.34)$$

so that

$$f'(\psi) = 1 - e \cos \psi. \quad (2.35)$$

Explicit substitution of equations (2.34) and (2.35) into (2.32) gives

$$\begin{aligned} \psi_{i+1} = \psi_i - [\psi - \psi_0 - e \sin \psi + e \sin \psi_0 - 2\pi(t-t_0)/\tau] \\ / [1 - e \cos \psi_i]. \end{aligned} \quad (2.36)$$

It is easy to show (Hildebrand p. 575f) that the difference of ψ_{i+1} and ψ_* is proportional to the square of the difference of ψ_i and ψ_* :

$$\psi_* - \psi_{i+1} \approx -[f''(\psi_*)/2f'(\psi_*)] (\psi_* - \psi_i)^2. \quad (2.37)$$

As long as $|\psi_* - \psi_i| < 1$, convergence will occur.

The hybrid technique presented above performed very well. There was not a single instance of the program

failing to find the true anomaly. In addition, over 2×10^6 tests of this method with $e=0.999$ have been performed without a single failure indicating that an excellent method of solution has been found. After performing five successive substitutions, the technique required typically three or four iterations of the Newton-Raphson technique before $|\psi_* - \psi_i| < 10^{-10}$. All in all, the technique is quite satisfactory.

2.5. Kinetic Energy at Infinite Separation

One of the quantities of interest after a collision is the kinetic energy of each of the subsystems (single or binary) when it is effectively out of range of the other surviving subsystems. Since the FBP has no analytic solution, we must make approximations to it if we are to find these kinetic energies as the separations become infinite.

The only situation involving gravitational motion for which it is possible to find the exact kinetic energies of the objects at infinite separation given conditions at finite separations is the two-body case. Consider two unbound masses m_1 and m_2 separated by a distance r and moving with relative speed V . If the two objects interact only gravitationally, the total energy of the system in relative coordinates is

$$E = \mu V^2/2 - k/r \quad (2.38)$$

where μ is the reduced mass and $k=Gm_1m_2$. If we call the relative speed at infinite separation V_∞ and the speed of m_i ($i=1,2$) at infinite separation in the center-of-mass reference frame $v_{i\infty}$, then

$$m_i v_{i\infty} = \mu V_\infty. \quad (2.39)$$

If we square equation (2.39) and divide by $2m_i$, we find

$$m_i v_{i\infty}^2/2 = (\mu^2/m_i) V_\infty^2/2. \quad (2.40)$$

This gives

$$KE_{i\infty} = (\mu/m_i) E \quad (2.41)$$

where $KE_{i\infty}$ is the kinetic energy of the i -th mass when the separation is infinite. Equation (2.41) can be written in a slightly more useful form if we define v_i as the speed of the i -th particle at finite separation in the center-of-mass reference frame. Application of the distributive law of multiplication over addition to equation (2.38) as well as utilization of v_i results in

$$m_i v_{i\infty}^2/2 = \mu v_i^2/2 - (\mu/m_i) k/r; \quad (2.42)$$

therefore, the potential energy partitions as μ/m_i .

In practice, equation (2.42) was used to find the kinetic energy of a subsystem (single or binary) when removed to infinity with respect to the coordinates of the center of mass of the remaining subsystems. While this is only an approximation for the FBP, it appears to be the best

approximation available in the absence of unlimited computer time.

CHAPTER 3

THE PROGRAM

3.1. Introduction

This computer experiment of numerical simulations of collisions between two binary stars was carried out by a computer program which was executed on several different computers. The program initialized the collisions, solved the equations of motion, and then tabulated the results; thereby it performed the duties of "experimental setup." The program's central role in the completion of this dissertation warrants a discussion of the techniques incorporated into it as well as the organization of the collisions.

3.2. Organization of Collisions

Collisions were performed in groups with members of the same group having identical masses, initial orbital eccentricities, impact parameters, initial ratio of binary binding energies (β), and collision energies (α). The quantities which were varied within a given group by Monte Carlo sampling are several of the orbital elements of each binary. They are: the orbital inclinations, the arguments of periastron, the longitudes of the ascending nodes, and the mean anomalies. These quantities were determined by a

pseudo-random process for each binary in each collision. Typically, a group contained 200 collisions although groups of hard collisions ($\alpha < 1$) often contained fewer.

When the simulation of the collisions in a group was completed, the data were tabulated. The quantities which were tabulated are: the total "macroscopic" kinetic energy of the surviving components of the system, the total binding energy residing in binaries, the average eccentricity of the surviving binaries, the distance of closest approach during each collision, and the time span of each collision. Also of interest was the final configuration of the system--which stars were components of binaries and which were single stars. These quantities were summarized in a single-page report produced at the end of each group of runs. A typical run summary is shown in Figure 1 and the results of a completed collision followed by an uncompleted collision are shown in Figure 2.

3.3. Initializing a Collision

After the appropriate orbital elements were found and Kepler's Equation was solved by the method presented, the cartesian coordinates (both position and velocity) of each mass were found. This was accomplished by the standard transformation from the orbital elements and the true anomaly to cartesian coordinates as given in Bate, Mueller, and White (pp. 71-83). At this point the binaries exist "on top of each other." They must be separated into independent

BINARY 1		BINARY 2	
M1 =	1.000000E 00	M3 =	1.000000E 00
M2 =	1.000000E 00	M4 =	1.000000E 00
E1 =	0.000000E-01	E2 =	0.000000E-01
RATIO OF BINDING ENERGIES =		1.0000	
IMPACT PARAMETER =		.5000	
RATIO OF KE TO BE =		5.0000	
NUMBER OF ATTEMPTED COLLISIONS =		200	
PERCENT COMPLETED =		100.0000	
PERCENT FAILED =		.0000	
- ENERGY =		.0000	
- STEPS =		.0000	

QUANTITY	MEAN	SD	SE
BINDING ENERGY	5.204600E-01	3.549940E-01	3.187940E-02
KINETIC ENERGY	4.327240E 00	3.814630E-01	2.697350E-02
ECCENTRICITY	6.952500E-01	2.163770E-01	1.943120E-02
CLOSE APPROACH	1.748480E-01	1.099060E-01	7.771529E-03
TIME/TREF	2.941920E 01	1.062860E 02	7.515560E 00
STEPS	9.355000E 02	4.365979E 02	3.087210E 01

FINAL STATES					
STATE				NUMBER	PERCENT
1	2	3	4	76	38.0000
12	3	4		49	24.5000
13	2	4		6	3.0000
14	2	3		2	1.0000
1	23	4		0	.0000
1	24	3		3	1.5000
1	2	34		36	18.0000
12	34			27	13.5000
13	24			0	.0000
14	23			1	.5000

Figure 1. A typical run-summary for a group of collisions.

2

COLLISION INCOMPLETE

TRINARY FORMED

SINGLE 1 KINETIC ENERGY = 1.419967E-01
 TRINARY 24 3 KINETIC ENERGY = 1.982828E-02 BINDING ENERGY = 4.290820E-01 ECCENTRICITY = 8.687619E-01
 BINDING ENERGY = 6.224140E-01 ECCENTRICITY = 4.575361E-01
 50000 STEPS ENERGY ERROR = 1.125432E-05 RMIN = 3.245555E-03 TIME (YEARS) = 1.050832E 02

1.989000E 33 1.484807E 13 -1.292978E 12 2.674801E 13
 9.365207E 06 -1.910742E 06 1.800968E 07

5.967000E 33 -1.839042E 12 5.475725E 11 -4.029964E 12
 -6.122311E 06 8.906245E 05 -1.583233E 07

1.989000E 33 -2.058848E 12 -1.850179E 11 -4.348999E 12
 -1.054117E 07 3.902918E 06 2.692133E 07

5.967000E 33 -2.424031E 12 -5.490725E 10 -3.436374E 12
 6.514300E 06 -1.554683E 06 8.553213E 05

27

3

COLLISION COMPLETED

BINARY 1 4 KINETIC ENERGY = 1.091557E-01 BINDING ENERGY = 9.614420E-01 ECCENTRICITY = 6.380477E-01
 SINGLE 2 KINETIC ENERGY = 4.384386E-02
 SINGLE 3 KINETIC ENERGY = 1.101528E-01
 5250 STEPS ENERGY ERROR = 1.525108E-04 RMIN = 1.882740E-01 TIME (YEARS) = 1.398950E 02

Figure 2. Two samples of collision results.

binaries and given the appropriate center-of-mass positions and velocities; they must be made to collide. These center-of-mass quantities were not found randomly, but from the initial kinetic energy and the impact parameter, two of the quantities which define a group.

After the above procedures were performed and the cartesian positions and velocities were found, the system was in a form appropriate for computer solution of the equations of motion. Control of the program then passed to the integration routine.

3.4. The Integration Routine

The integrator used to solve this problem was developed to solve the equations of motion for just such a system and to reduce the difficulties previously outlined. Its purpose is to simulate collisions between binary stars; however, if implemented appropriately, it can be generalized to trace the dynamical evolution of a cluster of stars.

The equations of motion were regularized as described so that the integrator could solve them accurately during close approaches. This transformation was accomplished immediately after entering the integrator. Upon leaving, a transformation back to normal, physical space and time was effected. Thus the integrator dealt almost exclusively with the regularized quantities.

The routine which actually solved the equations of motion uses the fourth-order Adams-Moulton predictor-

corrector integrator which is started by a fourth-order Runge-Kutta integrator. One of the advantages of using a predictor-corrector integrator is that an indication of the error introduced by the integrator can be obtained from a comparison of the predicted with the corrected values. An estimate of that error is (Bate, Mueller, and White pp. 414-420)

$$\epsilon = 19/270 |x^P - x^C|. \quad (3.1)$$

x^P is the predicted result and x^C is the corrected result. If the error, ϵ , exceeds some upper limit, the time step may be reduced, while it may be increased if ϵ becomes less than some lower limit. The first time a particular collision was performed, the upper and lower limits on ϵ were 10^{-6} and 10^{-8} , respectively. If, during the course of integration, the relative energy error exceeded 10^{-2} , the collision was restarted from the beginning with the limits on ϵ reduced by a factor of 10^{-4} . If this limit was exceeded again, the collision was again restarted with the limits on ϵ further reduced. This was repeated until either the collision was completed or three attempts were exhausted. If the latter situation occurred, an attempt was made to find the intermediate configuration and the energy of each component of the system after which the collision was aborted. The lowest limits on ϵ were 10^{-14} and 10^{-16} . At this level, the number of integration steps required to complete the collision becomes prohibitive even for a relatively simple collision.

As mentioned previously, one of the major problems plaguing this problem is the formation of quasi-stable systems involving binaries. The integrator developed reduces this problem by treating each tightly bound binary as a single star when other members of the system are distant enough to give Q in excess of 10^5 . The components of the system were checked every 20 integration steps to ascertain whether any binaries should be reduced or any reduced binaries should be resolved. In either case, the appropriate remedial measures were taken and the integration routine continued solving the modified equations of motion of the system.

3.5. The Beginning and Ending of a Collision

A collision such as the ones with which we are concerned theoretically requires infinite real time to complete if we ignore the finite lifetimes of the stars. Clearly we cannot run the simulation for even a fraction of that time; certain sacrifices in the form of approximations must be made. A requirement for the use of an approximation such as reduction is that it be applied consistently. We have made every effort to do just that, even when beginning and ending a collision, as will now be illustrated.

The separation of the binaries at the beginning of a collision is determined through the reduction process with the requirement that $Q=10^5$ (equations (2.20)-(2.23)). For equal mass binaries composed of equal mass stars with equal

separation, the initial separation of the binaries is 92.8 times the separation of the components of either binary. This initial separation is somewhat more stringent than that used in previous work by Hills (1975), who somewhat arbitrarily chose a factor of 60 for all cases. According to our criterion, he should have used a factor of 73.6 for the equal mass case. If such a technique is used to find the initial separation of the binaries, then the reduction approximation contributes a term to the total error that is typical of the error contributed by beginning a collision at finite separation.

A major logical problem in this computer experiment was deciding when a collision is effectively finished. For a stable final configuration, the collision must be carried out for a sufficient enough time so the final products do not interact with each other sufficiently to appreciably change the final results. Thus we have developed a set of tests to apply to each subsystem to ascertain whether the collision is to be terminated. A collision is terminated when four conditions are simultaneously met:

1. Each star is energetically either a single star or a component of a binary;
2. Each binary has $Q > 10^5$;
3. Each subsystem is energetically unbound to all possible combinations of the remaining subsystems;

4. Each subsystem is moving away from all other subsystems.

Determining whether a given star is a member of a binary is similar to deciding whether a binary is to be reduced to a single star. If the star has a negative energy with respect to another star, then the two stars form a binary. The binary is considered far enough from all other subsystems if Q for that binary exceeds 10^5 . When all stars are single or are members of relatively isolated binaries, we have completed tests 1 and 2. We now move on to test 3.

Testing the energy of a subsystem relative to all other subsystems is very simple. Consider the subsystem to be tested. Compute the total energy of it with respect to all possible combinations of the remaining systems. If all energies are positive, the system passes test 3.

This leaves us with test 4. This test is also quite simple to carry out. Again consider the subsystem to be tested. For all possible combinations of the remaining subsystems, compute the coordinates of the center of mass. If the two subsystems (the subsystem to be tested and the subsystem composed of combinations of the remaining subsystems) are moving apart, the inner product of the relative velocity and the relative position is positive and the subsystem to be tested passes test 4.

When each subsystem passes each of the above tests, the collision is over and the various energies and other parameters are tabulated. It is difficult to ascertain

whether these tests will be passed only by stable systems.
I suspect not, but I have not imagined a case these tests do
not cover.

CHAPTER 4

ANALYSIS OF RESULTS

4.1. Introduction

In performing this computer experiment, we have simulated 41,564 collisions between pairs of binary stars, thereby producing prodigious amounts of data. Extracting a considerable portion of the possible generalizations and conclusions from this data could require years. We cannot do this here. Instead, we will reduce the data to a fairly concise form, a series of plots of the quantities given in Appendix A, and then draw some very general conclusions regarding this experiment.

The set of quantities we will consider in this analysis will be divided into three categories: the exchange of energy; the final configuration (which stars are single and which are components of a binary) of the system; and other, miscellaneous quantities such as the average eccentricity of the surviving binaries and the average distance of closest approach. These quantities in no way exhaust the set of those that might be tabulated, however, if we understand the relationship of these quantities to the independent parameters, we probably have a good understanding of the dynamics of collisions between two binary systems.

4.2: The Exchange of Energy

4.2.1. Introduction

When a binary star becomes more tightly bound because of a collision with another star or with a group of stars, it gives up its orbital energy to the other stars. The energy released or absorbed through a collision may be the most important quantity obtainable from this experiment since the dynamical structure of a group of stars is extremely dependent upon the available kinetic energy.

Since each of these collisions conserves energy, the kinetic energy added to the stellar system in which the two colliding binaries are imbedded divided by the initial total binding energy of the binaries, ξ , (hereafter relative energy exchanged) is equal to the relative binding energy increase of the surviving binaries as the separations of the unbound products become infinite. The total energy may be decomposed into two terms, E_{ext} and E_{int} , the total macroscopic energy and the total internal energy of the binaries, respectively. From conservation of energy, the total energy before the collision

$$E = E_{exti} + E_{inti} \quad (4.1)$$

equals the total energy after collision

$$E = E_{extf} + E_{intf}. \quad (4.2)$$

If we subtract equation (4.1) from equation (4.2) and divide by the initial total binding energy of the binaries, BE_i , we obtain

$$(E_{extf}-E_{exti})/BE_i + (E_{intf}-E_{inti})/BE_i = 0 \quad (4.3)$$

or

$$\xi = \Delta E_{ext}/BE_i = -\Delta E_{int}/BE_i \quad (4.4)$$

where $\Delta E_{ext} = E_{extf}-E_{exti}$ and $\Delta E_{int} = E_{intf}-E_{inti}$. The binding energy is the energy required to dissociate both binaries. We can therefore write

$$\xi = \Delta E_{ext}/BE_i = \Delta BE/BE_i \quad (4.5)$$

where $\Delta BE = BE_f - BE_i$. By examining the effect of a collision on the total binding energy of the four masses, we can find the kinetic energy released through the collision.

4.2.2. The Exchange of Energy at Zero Impact Parameter

In the upper graph in each of Figures 3-7, we show a plot of the exchanged energy (ξ) versus the common logarithm of α ($\log \alpha$) for one of the five families of collisions. (As a reminder, α is the initial kinetic energy of the binaries expressed in units of the minimum energy required to dissociate the binaries.) The impact parameter is zero for all cases. Each cross represents a data point and the vertical extent of the cross is the error associated with that datum. The curve drawn through the points as well as

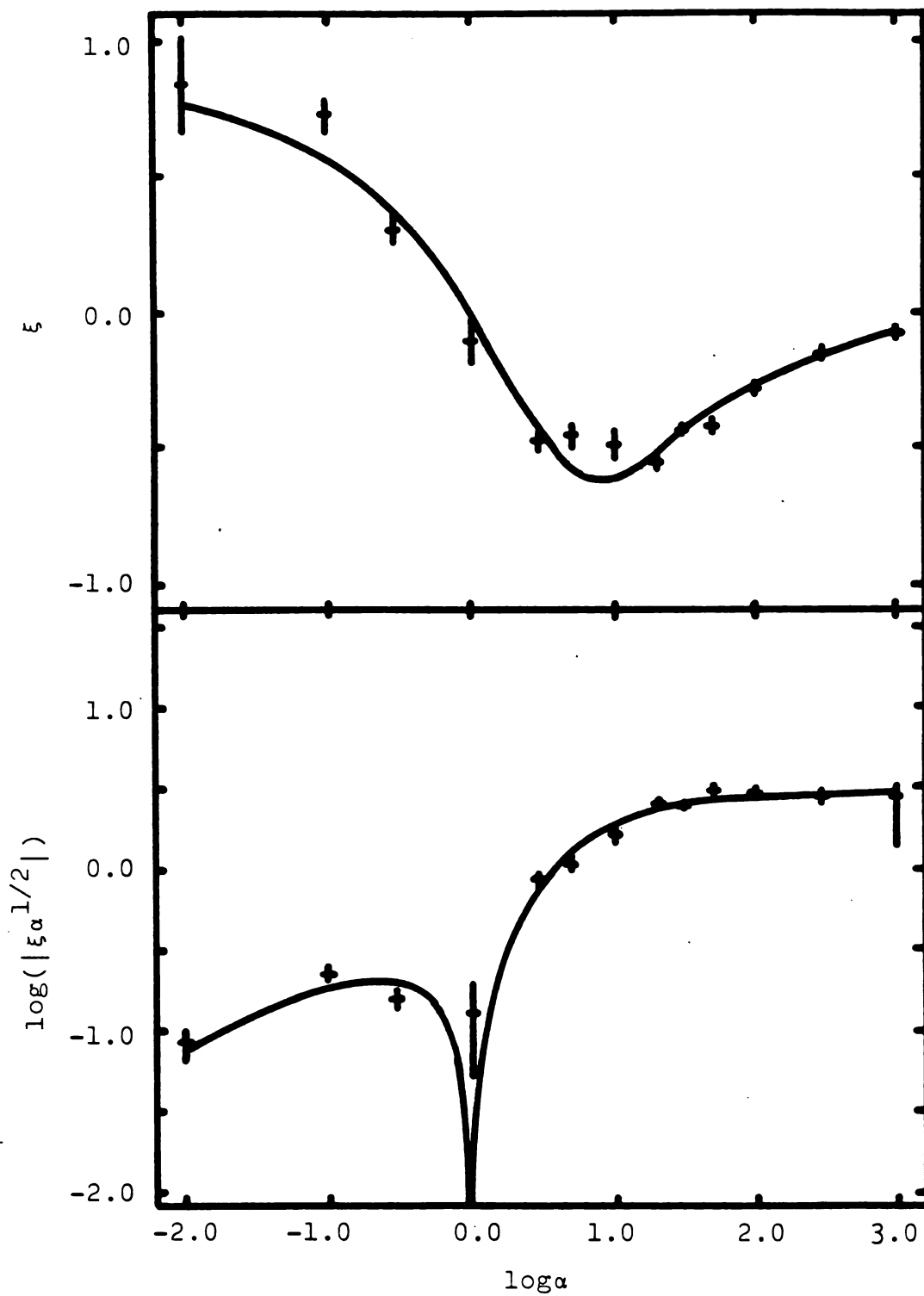


Figure 3. Plots of ξ and $\log(|\xi \alpha^{1/2}|)$ versus $\log \alpha$ for family A.

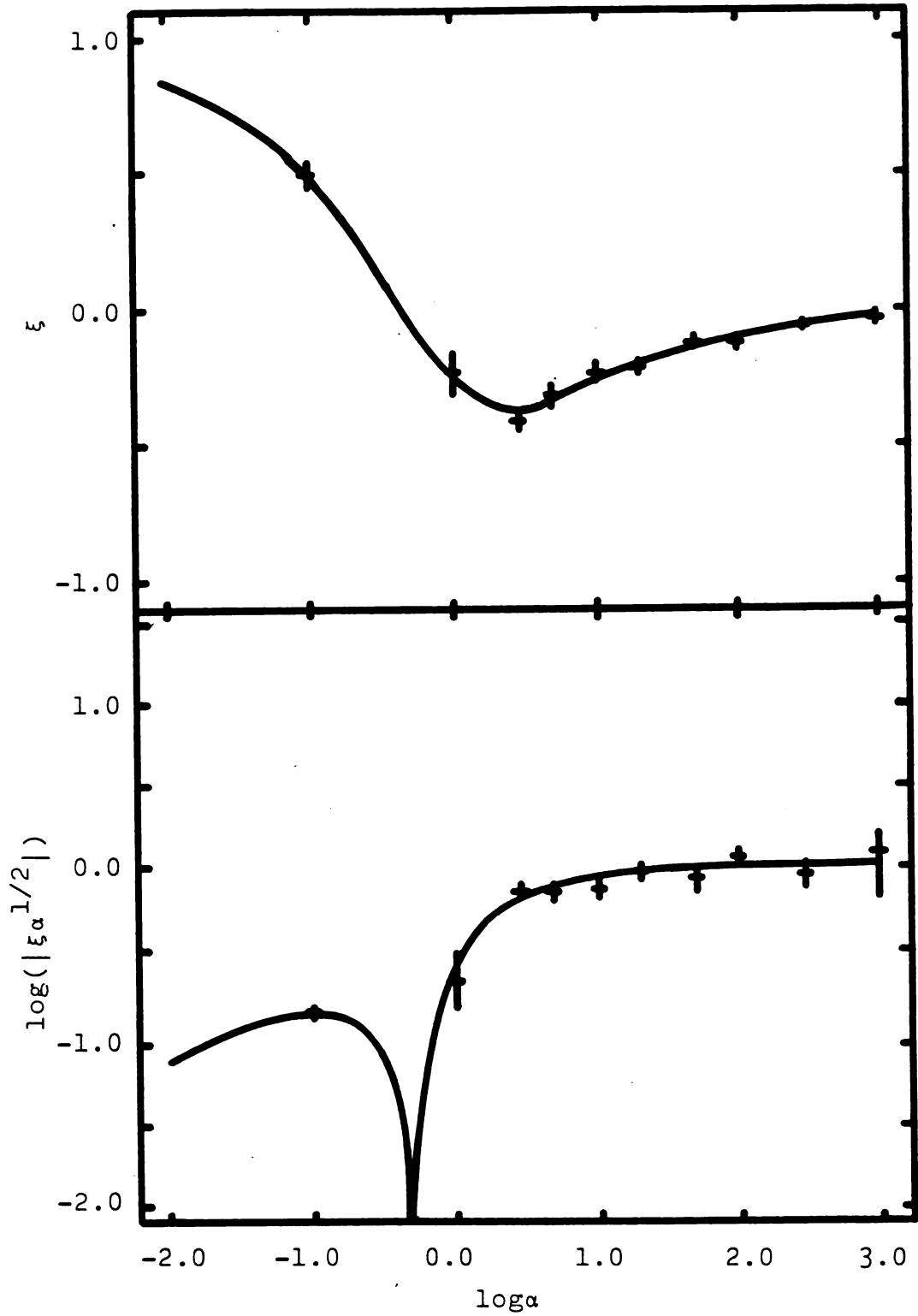


Figure 4. Plots of ξ and $\log(|\xi \alpha^{1/2}|)$ versus $\log \alpha$ for family B.

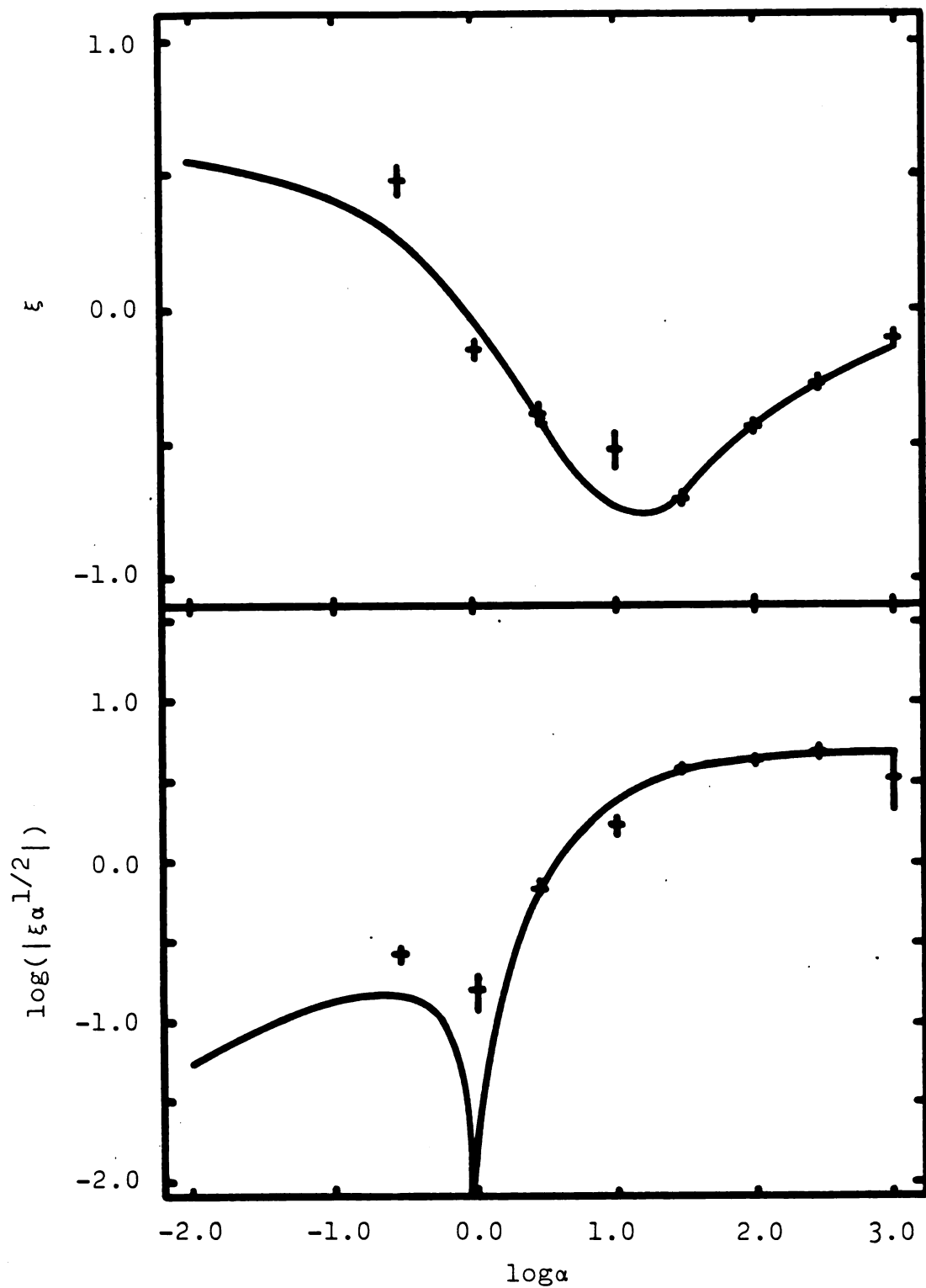


Figure 5. Plots of ξ and $\log(|\xi \alpha^{1/2}|)$ versus $\log \alpha$ for family C.

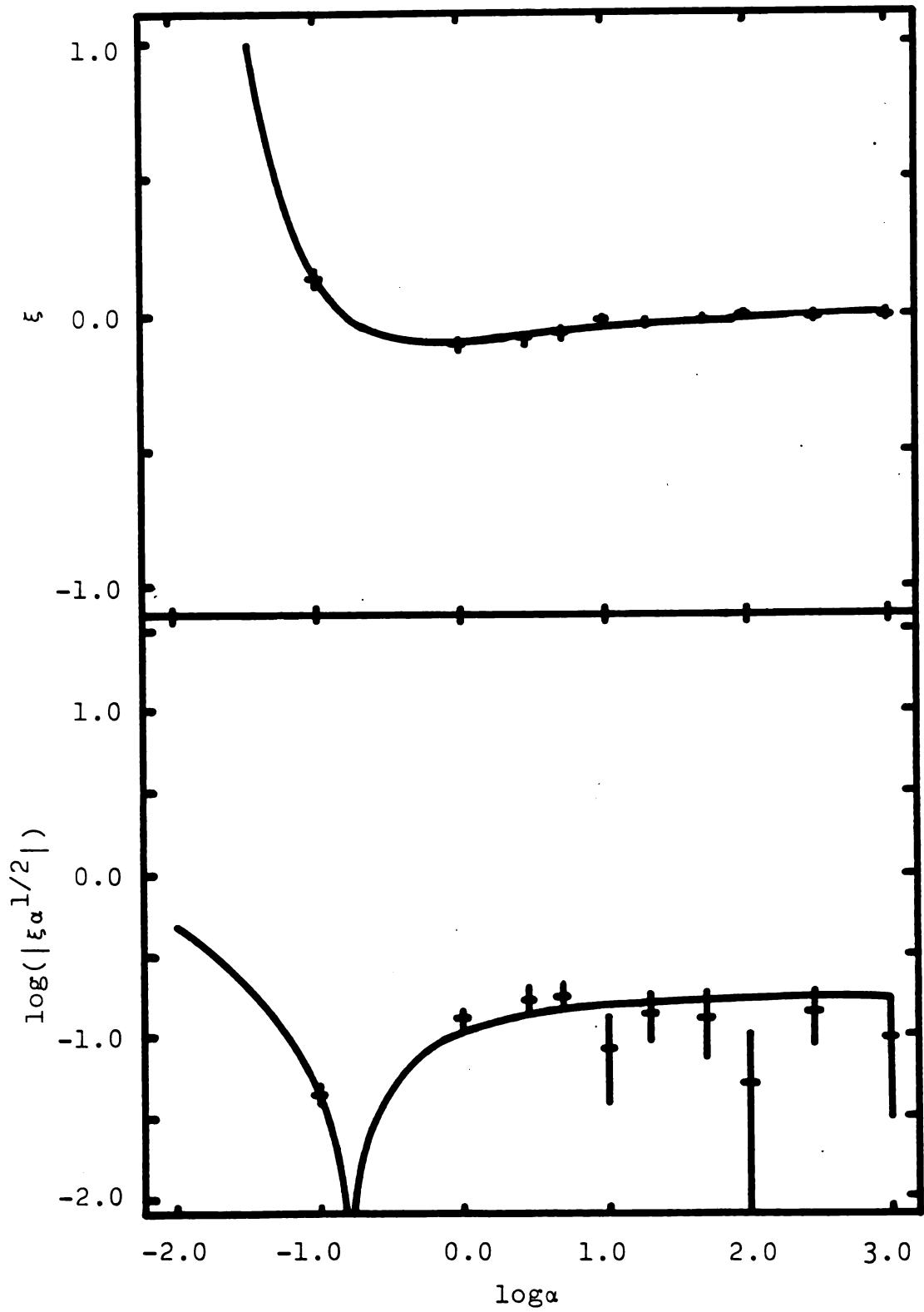


Figure 6. Plots of ξ and $\log(|\xi \alpha^{1/2}|)$ versus $\log \alpha$ for family D.

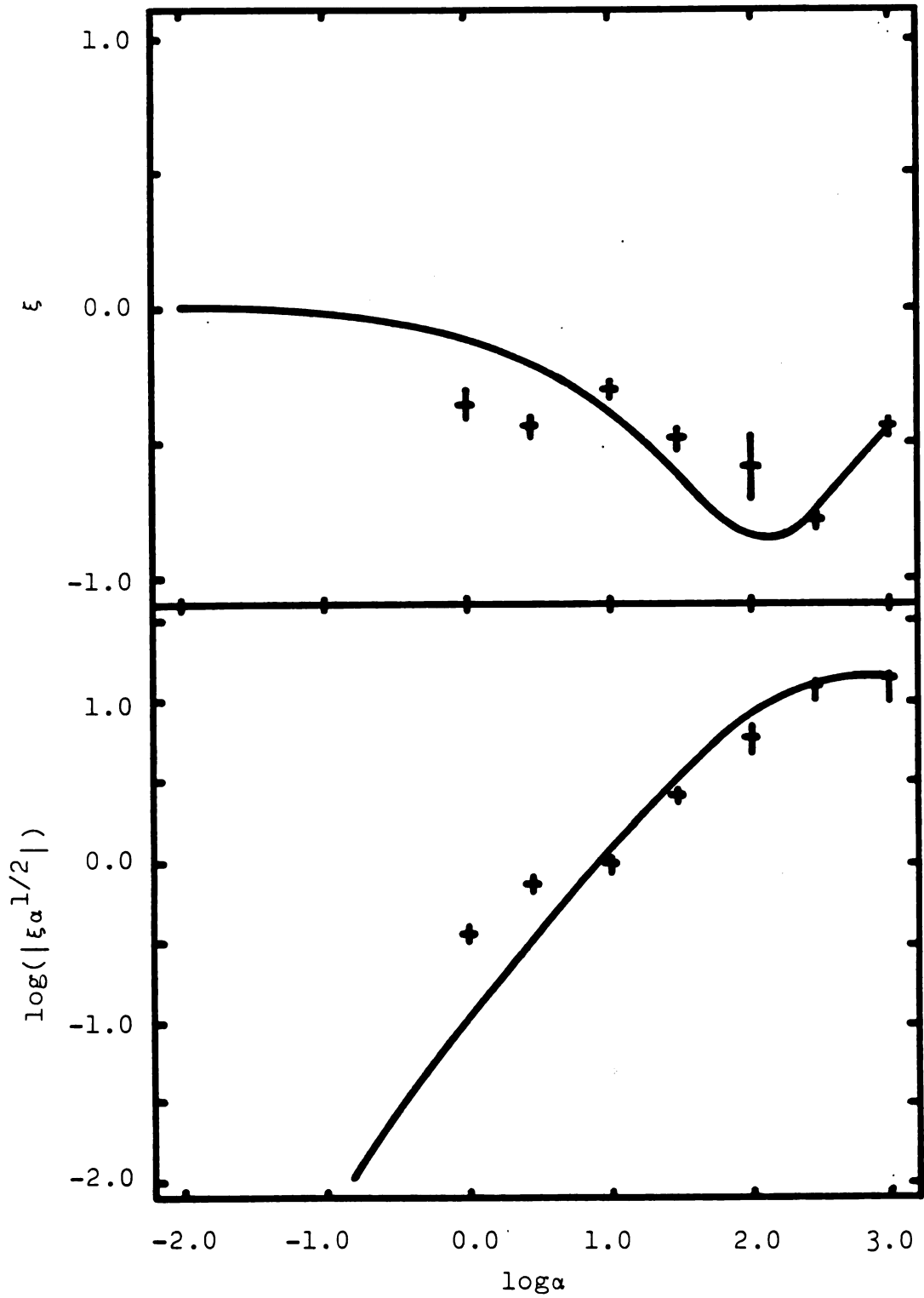


Figure 7. Plots of ξ and $\log(|\xi_\alpha^{1/2}|)$ versus $\log \alpha$ for family E.

each lower graph will be explained below. Even though these plots are quite complicated, we can make some general statements about them.

Each of the plots contains two regions, the region where $\xi > 0$ (small α) and the region where $\xi < 0$ (large α). We will call collisions with $\xi > 0$ "hard" collisions and those with $\xi < 0$, "soft." The point separating these two regions will be labeled $(\alpha_0, 0)$ since $\xi = 0$ at this point. α_0 is usually near unity.

In the extremely large- α region ($\alpha > 30$), we might expect ξ to vary roughly linearly with the time the binaries are close enough to interact with each other. If this is true, then $\xi \alpha^{1/2}$ should be roughly constant in this region. Taking this as a clue to possible later simplifications, we plot $\log(|\xi \alpha^{1/2}|)$ versus $\log \alpha$ for each family. This results in the lower plots in Figures 3-7. As expected, $\xi \alpha^{1/2}$ is approximately constant for $\alpha > 30$ for each of the plots with the remainder being surprisingly well-behaved.

As α approaches zero, we expect ξ to approach some finite, non-zero value (Hills 1975) requiring that $\xi \alpha^{1/2}$ vanish. In the region $0 < \alpha < \alpha_0$, $\xi > 0$ causing $\xi \alpha^{1/2} > 0$.

Any function which is to predict $\xi \alpha^{1/2}$ must increase from zero at $\alpha = 0$, peak, then decrease to negative values as α passes α_0 . It must then become constant and negative as α passes 30. A function possessing these qualities is

$$\xi \alpha^{1/2} = A[1 - \exp(-b\alpha)][(\alpha_0/\alpha)^{1/2} - 1] \quad (4.6)$$

as we will now verify. As α approaches zero, we have

$$\xi \alpha^{1/2} = Ab(\alpha \alpha_0)^{1/2} \quad (4.7)$$

so that

$$\xi = Ab\alpha_0^{1/2}, \quad (4.8)$$

a constant as expected. For extremely large α , we write

$$\xi \alpha^{1/2} = -A \quad (4.9)$$

or

$$\xi = -A/\alpha^{1/2}, \quad (4.10)$$

again, as expected. Of course, if $\alpha = \alpha_0$, then $\xi = 0$.

By choosing the parameters appropriately, equation (4.6) can be made to fit the boundary conditions given. We have accomplished this fit by using the method of least squares. Since equation (4.6) can not be made linear in the parameters, we used a grid search of parameter space to minimize χ_v^2 as given by Bevington (Chapter 11). The results of these fits are given in Table 1. The curves in Figures 3-7 are those generated by graphing equation (4.6) with the parameters appropriate for each family as given in Table 1. Although χ_v^2 is quite large for most of the families, the curves do appear to roughly fit the data.

In performing the least squares fits of the data to various curves, we minimized χ_v^2 in the form

Table 1. The results of least squares fits of the data to equation (4.6).

Family	A	b	α_0	χ_v^2
A	3.048	0.286	0.959	3.34
B	1.083	1.338	0.461	0.86
C	4.676	0.137	0.928	8.41
D	0.170	329.524	0.156	1.99
E	14.381	0.009	0.030	31.31

$$\chi_v^2 = 1/(N-n) \sum_{i=1}^N [y_i - y(x_i)]^2 / \sigma_i^2, \quad (4.11)$$

where N is the number of data points, n is the number of parameters in the fitting function $y(x)$, y_i is the i -th dependent data point, and x_i is the corresponding independent data point. σ_i is the standard error of y_i since each y_i is a mean obtained from roughly 200 data points. When defined in this manner, χ_v is approximately the root-mean-square of the standard scores of the data. We consider an excellent fit to occur when $\chi_v^2 < 1$ for the fit. This form of χ_v^2 is used throughout this dissertation.

4.2.3. The Exchange of Energy Versus Impact Parameter

The relationship between the exchanged energy and the impact parameter appears to be fairly simple. The exchanged energy (ξ) is roughly gaussian in the impact parameter (p):

$$\xi = \xi_0 \exp[-(p/p_0)^2], \quad (4.12)$$

where ξ_0 is the energy exchanged at zero impact parameter and p_0 is the width of the distribution. While the data do not follow this relationship exactly, they do follow closely enough for certain general features to be found.

In all fairness, we must criticize the present use of equation (4.12). Examination of the data reveals that a gaussian is probably not representative of the relationship between ξ and p ; the data have certain anomalies which preclude the validity of equation (4.12). For example, it is common to find a depression in the $|\xi|$ versus p curve about $p=0$. This depression occurs most frequently with family A. Usually a curve with no depression can be fit to the data within the given error limits leaving one to wonder whether the depression is simply a statistical fluctuation. To reduce this uncertainty, a significant increase in the number of collisions contributing to these points must be obtained. The high cost of performing these collisions which are at small α prevents us from resolving this uncertainty at this time. Another difficulty with using a gaussian is that, for some values of α , the exchanged energy

often changes sign as p becomes large.

Even though they will not predict either of the above behaviors, we will use fits to a gaussian to provide us, in a systematic manner, information regarding the width and the depth of the distribution for the energy exchanged. Since the gaussian has only these two parameters, it is ideally suited to give us this information. Other reasonable curves such as the sum of two gaussians have too many parameters for them to be fit to data consisting of only a few points. Preliminary investigations indicate that, when more data is available, the sum of two gaussians will be the curve used to fit the data at low kinetic energy.

We performed least squares fits of equation (4.12) to data of a given family with identical binding energy ratios (β) and identical kinetic energies (α). Families A and B (with $\beta=0.111$) are the only ones with extensive data for non-zero impact parameters so they are the only ones for which these fits were performed. The results are summarized in Table 2. As expected, χ_v^2 is quite large for several of the fits, however, enough give values which are less than or roughly equal to unity to indicate that the gaussian function can provide a reasonable fit to the data.

Since ξ_0 is the exchanged energy at zero impact parameter, it should be calculable from equation (4.6) and the data of Table 2. Coupled with a relation giving p_0 , these allow us to find an expression for the cross-section for energy exchange at any α for a given family.

Table 2. A summary of least squares fits of the data to equation (4.12).

α	ξ_0	ρ_0	σ_E	χ^2_ν	σ_{Eg}
FAMILY A: (1-1)-(1-1)					
1.01	-.300+-0.035	1.881+-0.076	-1.062+-0.210	22.494	-1.462
3.00	-.615+-0.018	1.599+-0.044	-1.572+-0.133	4.482	-1.586
5.00	-.513+-0.019	1.397+-0.047	-1.001+-0.103	.902	-0.897
10.00	-.554+-0.015	1.164+-0.039	-.750+-0.071	1.168	-0.689
20.00	-.527+-0.017	.822+-0.040	-.356+-0.046	2.330	-0.359
30.00	-.454+-0.012	.802+-0.031	-.292+-0.030	.701	-0.337
100.00	-.285+-0.011	.651+-0.032	-.121+-0.017	2.191	-0.142
300.00	-.139+-0.007	.667+-0.027	-.062+-0.008	.617	-0.056
1000.00	-.065+-0.006	.652+-0.030	-.028+-0.005	.356	-0.028
FAMILY B: (3-3)-(1-1)					
3.00	-.337+-0.028	1.384+-0.065	-.645+-0.113	3.890	-0.503
5.00	-.260+-0.027	1.272+-0.067	-.421+-0.088	2.829	-0.338
10.00	-.212+-0.026	1.037+-0.097	-.228+-0.070	1.842	-0.191
20.00	-.195+-0.020	.985+-0.077	-.189+-0.049	2.820	-0.163
50.00	-.115+-0.016	.696+-0.081	-.056+-0.021	.613	-0.076
100.00	-.101+-0.007	.726+-0.038	-.053+-0.009	.758	-0.055
300.00	-.035+-0.005	.757+-0.057	-.020+-0.006	.865	-0.020
1000.00	-.026+-0.003	.582+-0.047	-.009+-0.003	.484	-0.008

We have found that p_0 depends on α roughly as

$$p_0 = p_\infty + k/\log(\alpha+1). \quad (4.13)$$

p_∞ is the width of the ξ - p curve as $\alpha \rightarrow \infty$. Least squares fits of the data for families A and B give the parameters shown in

Table 3. A summary of least squares fits of the data in families A and B to equation (4.13).

Family	p_∞	k	χ_v^2
A	0.5679	0.4584	0.035
B	0.4411	0.6033	0.006

Table 3. The χ_v^2 given in Table 3 were calculated with the errors in α , σ_α , set equal to unity since α is an input parameter and is taken to be exact. The fits appear to be quite good.

4.2.4. The Exchanged Energy Cross-Section

As a measure of the total effectiveness in releasing energy of a set of collisions from the same family with the same α and β , we will define the exchanged energy cross-section:

$$\Sigma_E = \frac{\text{total energy released}}{\text{energy incident per area}}. \quad (4.14)$$

Of course, we would like to find a form for equation (4.14) that we can use for computational purposes.

Consider a single binary acted upon by a beam of binaries which interact with only the target binary. The total binding energy of each binary in the beam and the target binary is E . The kinetic energy added to the two binary system by the collision is ΔE and the beam has a cross-sectional surface number density of binaries, n . With these definitions, we can write

$$\Sigma_E = 2\pi n \int_0^{\infty} \Delta E b db / nE \quad (4.15)$$

where b is the impact parameter. Since the units of b have not yet been specified, let us define a unitless impact parameter $p=b/a$ (the impact parameter actually used in the experiment) and a corresponding unitless cross-section $\sigma_E = \Sigma_E / \pi a^2$. We can then write

$$\sigma_E = \Sigma_E / \pi a^2 = 2 \int_0^{\infty} \xi p dp. \quad (4.16)$$

We can obtain an analytical expression for the cross-section by substituting for ξ from equation (4.12):

$$\sigma_E = 2\xi_0 \int_0^{\infty} \exp[-(p/p_0)^2] p dp \quad (4.17)$$

which integrates to

$$\sigma_E = \xi_0 p_0^2. \quad (4.18)$$

In practice, we have computed the cross-section by two different techniques. We used equation (4.18) with the data in the third and fourth columns of Table 2 as well as plotting the data points $(p, \xi p)$ manually on graph paper, drawing a smooth curve through the points, and integrating by counting the squares under the curve. Cross-sections computed by both of these techniques (σ_E and σ_{Eg} , respectively) are given in Table 2.

We have now developed all the tools necessary to give an expression for the cross-section for any α for families A and B. By combining equations (4.6), (4.13), and (4.18), we can write

$$\begin{aligned} \sigma_E = & A[1-\exp(-b\alpha)][(\alpha_0/\alpha)^{1/2}-1] \\ & \times [p_\infty + k/\log(\alpha+1)]^2/\alpha^{1/2}. \end{aligned} \quad (4.19)$$

We can use this equation with the data in Tables 1 and 3 to obtain graphs of σ_E versus α for families A and B. Since p_∞ and k are similar for families A and B, we will assume they do not vary significantly for the other families and will use the average of the p_∞ for families A and B for these families. With this assumption, we can include graphs of σ_E for families C, D, and E. All of the graphs are shown in Figure 8.

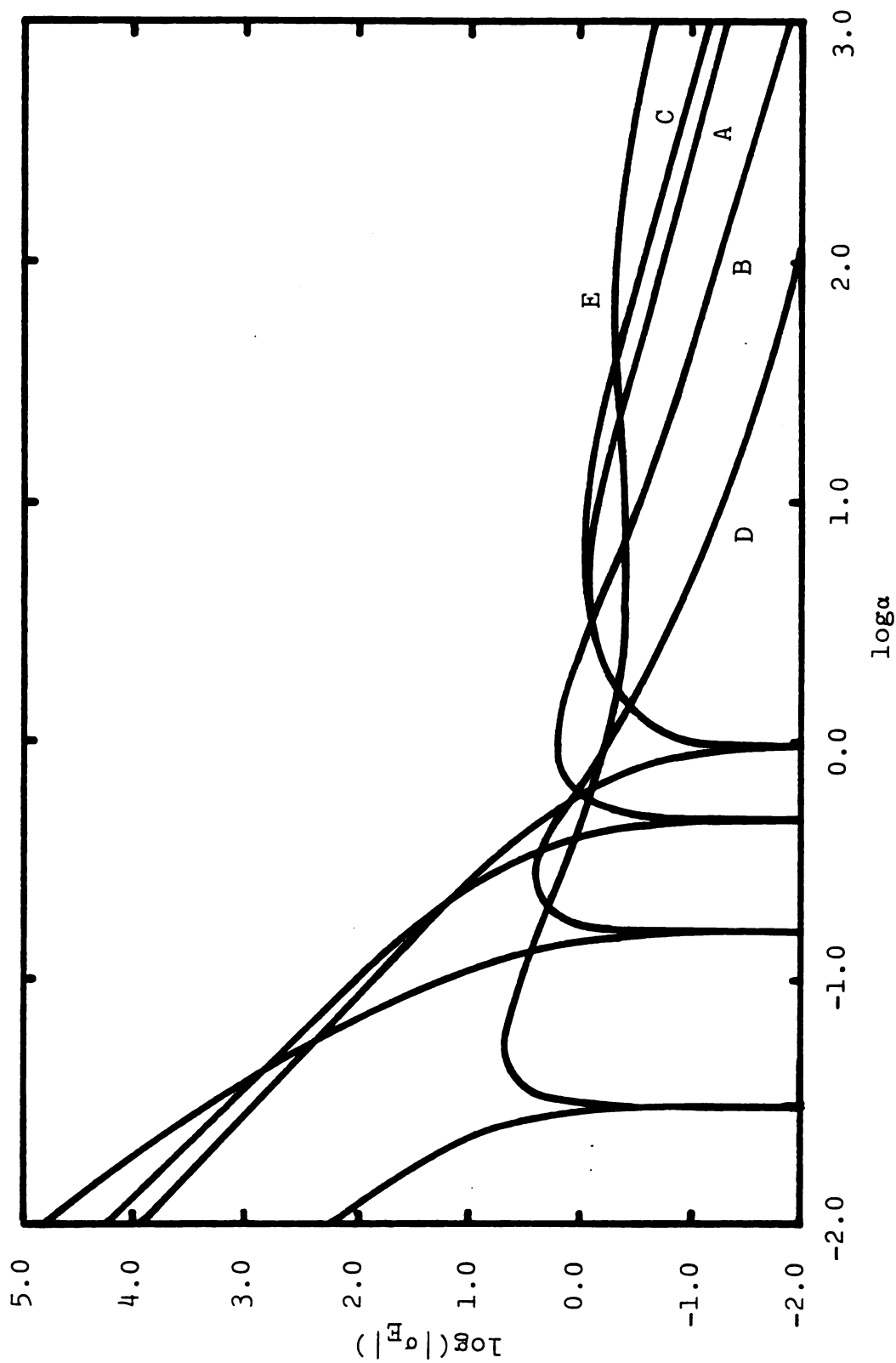


Figure 8. Plots of $\log(|\sigma_E|)$ versus $\log \alpha$ using equation (4.19) and the data from Tables 1 and 3.

4.3. The Final Configuration

When a collision has been terminated, we would like to find quantities such as the relevant kinetic and binding energies and the eccentricities of the surviving binaries. Before we can find these quantities, we must ascertain which stars are binary components and which are single stars; we must find the final configuration of the system. By tabulating the final configurations of a group of collisions, we can find the probability of occurrence of processes such as an exchange collision, complete dissociation of the system, and no change in the system. We will examine, in turn, each of the relevant quantities of the table in Appendix A.

First we will examine the probability of no change (PNC) occurring. In this case the surviving binaries are the same as the initial binaries, only the kinetic energies and the orbital elements change. Plots of PNC versus $\log \alpha$ are given in Figure 9. The plot for each family hovers near zero when $\log \alpha < 1$. In this region, virtually all "memory" of the initial configuration is lost. Then, as α increases past unity, the plot for each family, except family E, increases, reaching at least 0.845 when $\log \alpha = 3$. Beyond this we have not investigated.

Another way of forming two surviving binaries is through an exchange collision whereby the two surviving binaries are not the initial ones, but are composed of a different

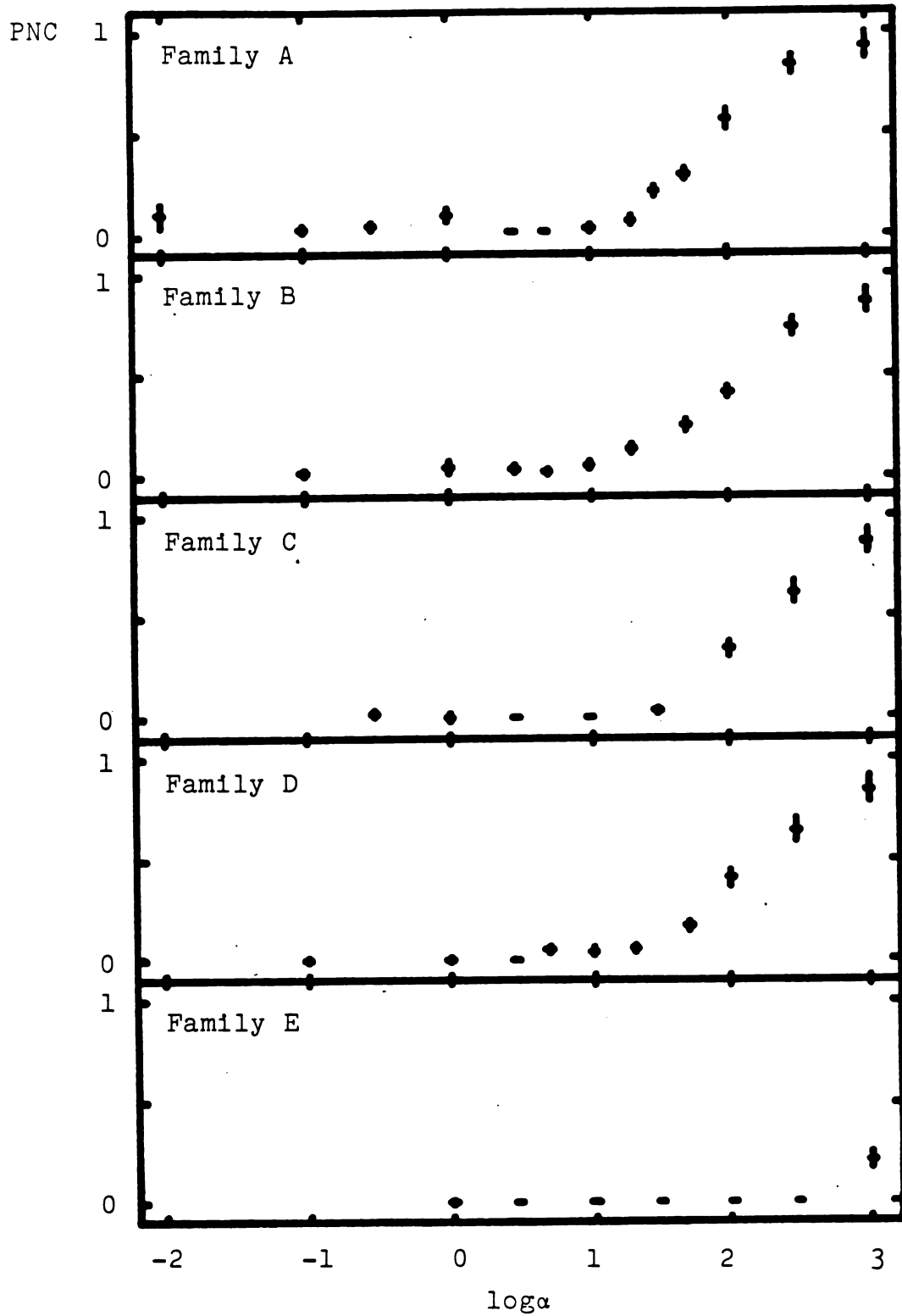


Figure 9. Probability of no change versus $\log \alpha$.

combination of stars. For binary-binary collisions, this implies that an exchange collision has taken place. When the masses of the stars are identical, the exchange collision is not important, but when each star has a distinct mass, it becomes interesting and potentially very important (Hills 1977). Plots of the probability of exchange (PE) versus $\log \alpha$ for the five families are given in Figure 10. As expected, there is a much higher incidence of exchange collision for families with binaries having a large difference in their component masses (families C and E) than for families with binaries having identical mass components. However, the explanation of this effect is not the usual one. One might expect exchange collisions for families C and E to result in a binary containing the two most massive stars. This does not occur because in the region where exchange collisions become important, α is too large for the system to reach any degree of dynamical equilibrium as required for the usual argument giving the ejection of the lightest stars. In fact, most of the exchange collisions (75% at $\alpha=1.01$ increasing monotonically with α for family C and 100% for all α for family E) were simply an exchange of the lighter components. This is not really surprising since it is much easier to change the course of a less massive star than of a more massive star.

Quite often only a single binary will survive the collision. Figure 11 summarizes the probability that this occurs (PSB) for each of the families of collisions. These

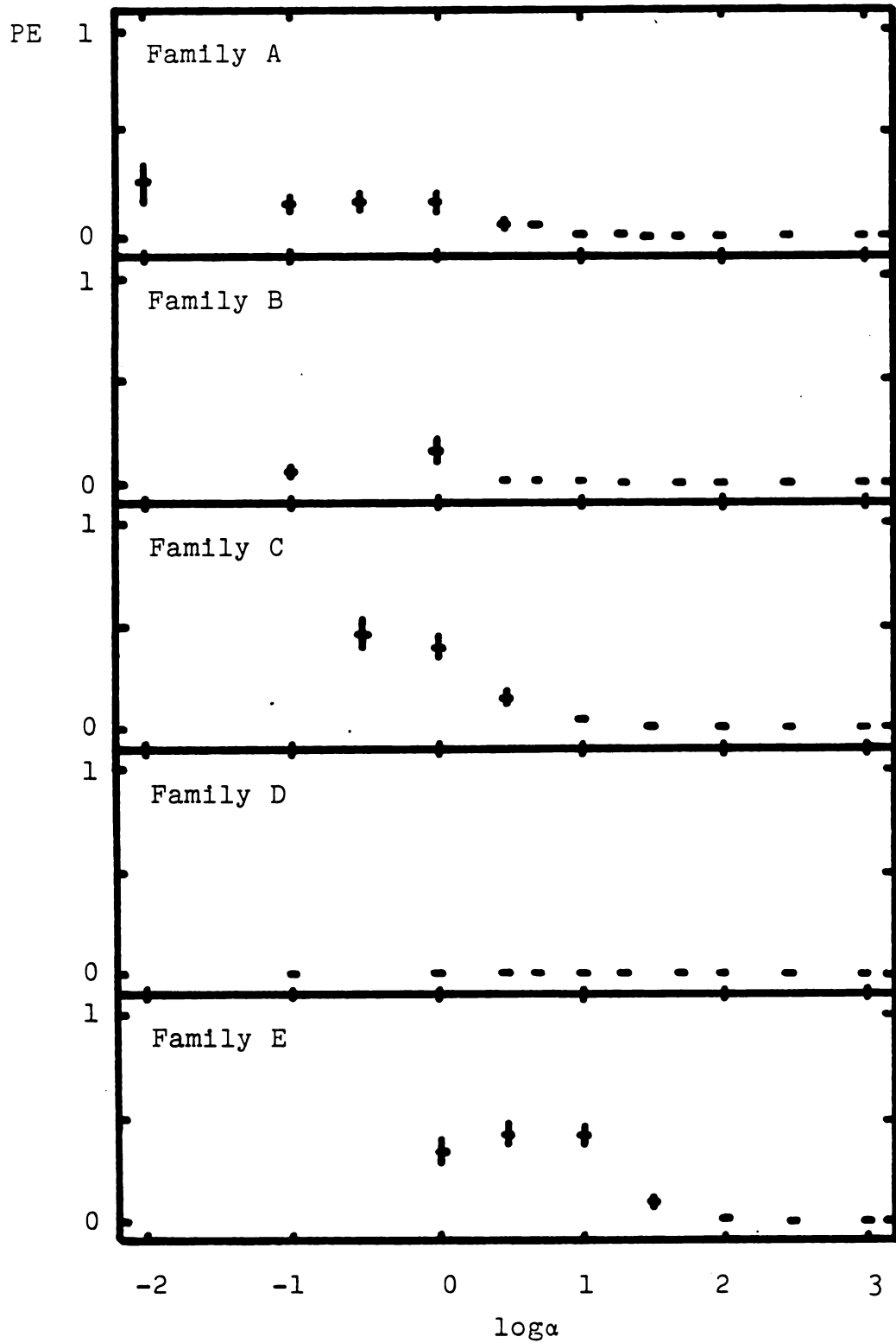


Figure 10. Probability of exchange versus $\log \alpha$.

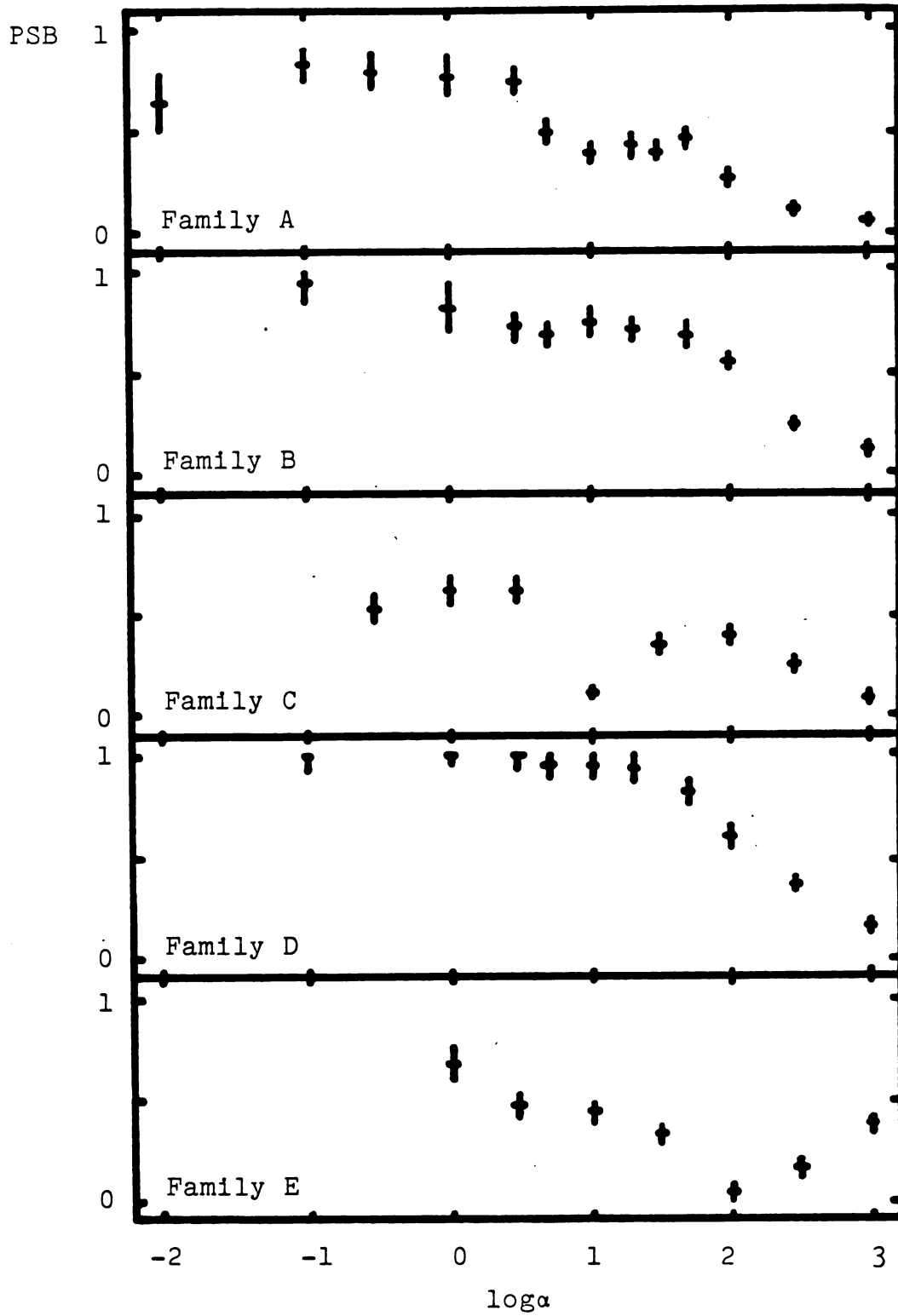


Figure 11. Probability of a single binary versus $\log \alpha$.

plots are somewhat erratic making it difficult to draw many general conclusions from them, but we can describe their general forms. The plots for families C and E reach a local minimum in the range $\alpha=10-100$ after which they peak and then, at least for family C, asymptotically decrease to zero. Presumably the plot for family E would also exhibit this behavior were the data extended to larger α . The plots for families B and D are at a plateau until α exceeds approximately 50 where they both asymptotically approach zero. Family A, not surprisingly, appears to be a hybrid of the C-E and the B-D cases. The low- α plateau gives way to a lower plateau when α exceeds three. This plateau exists until α exceeds 50 where the plot asymptotically approaches zero.

We will now examine the last possible final configuration of the system, that of complete dissociation (PD) or the formation of four single stars. The plots in Figure 12 summarize the dependence of PD on $\log\alpha$ for the five families of collisions. A feature we should note is that, for all families, $PD=0$ when $\alpha<1$. This is reassuring since the total energy ceases to be positive in this region thereby precluding complete dissociation of the system. Upon comparing families A, C, and E, we find that PD increases with the difference in the component masses of the binaries, peaking at high values of α . It would be interesting to perform collisions between binaries with component mass ratios of 100 or 1000. Unfortunately, we have not done this here so we will not attempt to extrapolate these results to

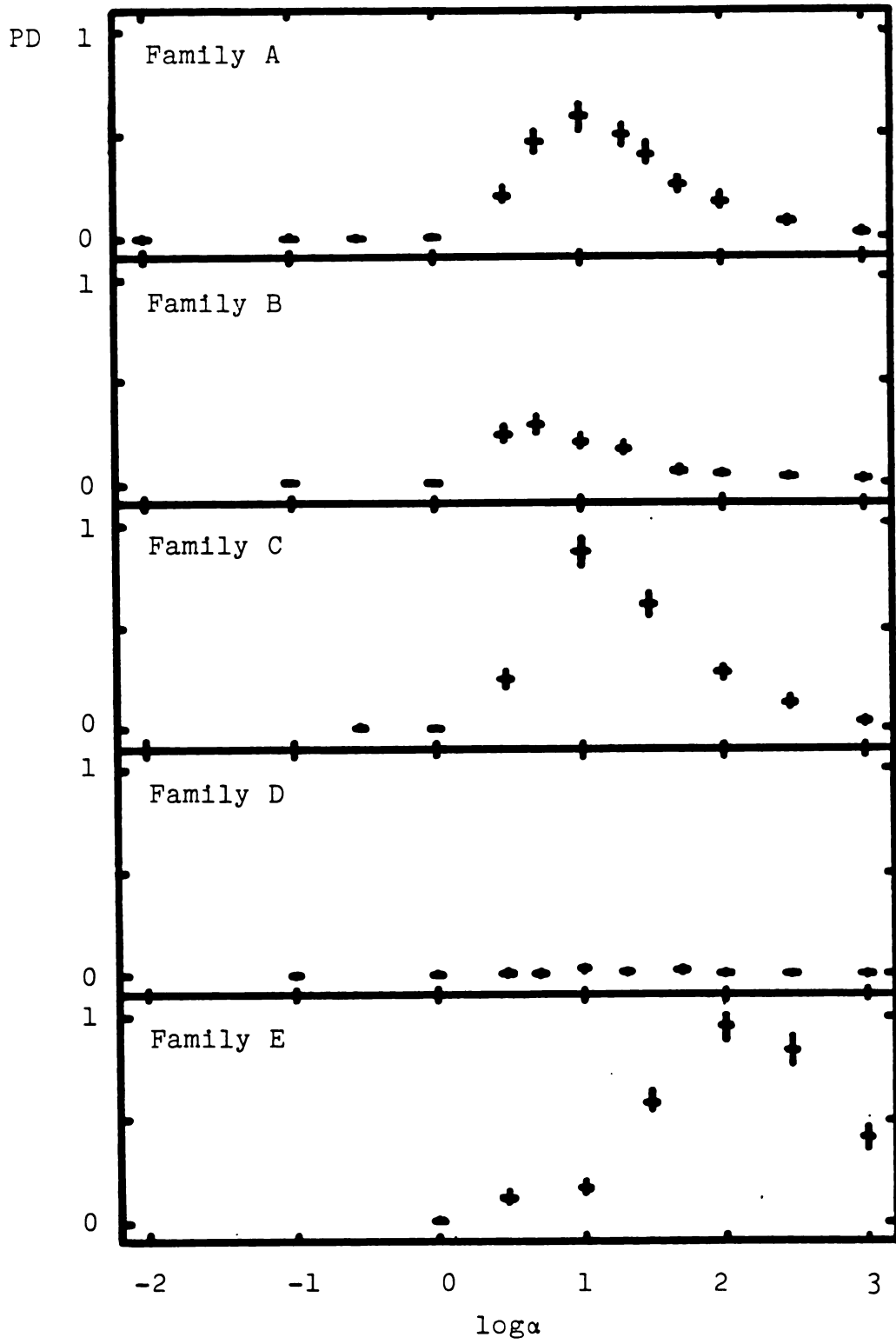


Figure 12. Probability of dissociation versus $\log \alpha$.

their asymptotic limits. We leave this to later experiments. When we compare families A, B, and D, we find that dissociation becomes extremely rare when the two most massive stars form a binary. We have already reached the asymptotic limit for these cases.

4.4. The Average Eccentricity of the Surviving Binaries

It has been postulated (Hills 1977) that the eccentricity of a binary can give a clue to its origin. One with a high eccentricity ($e > 0.5$) was probably formed by an exchange collision between a binary and a single star. We will now examine the average eccentricity of the binaries surviving the collisions between two binaries.

The data regarding the average eccentricity of the surviving binaries when the collision impact parameter is zero are summarized by the plots of Figure 13. As one might expect, when α is small, the average eccentricity is near $2/3$. This is the average eccentricity expected for a group of binaries in statistical equilibrium. The departure of family D from this "rule" is not surprising since the massive binary should, on the average, be affected little by colliding with a binary of one-tenth its mass. For each family except family D, the peak eccentricity occurs for fairly large α . The error bars indicate these are real peaks, not just statistical fluctuations. By comparing the peaks for families A, C, and E, one finds that the height of the peak increases as well as shifting toward increasing

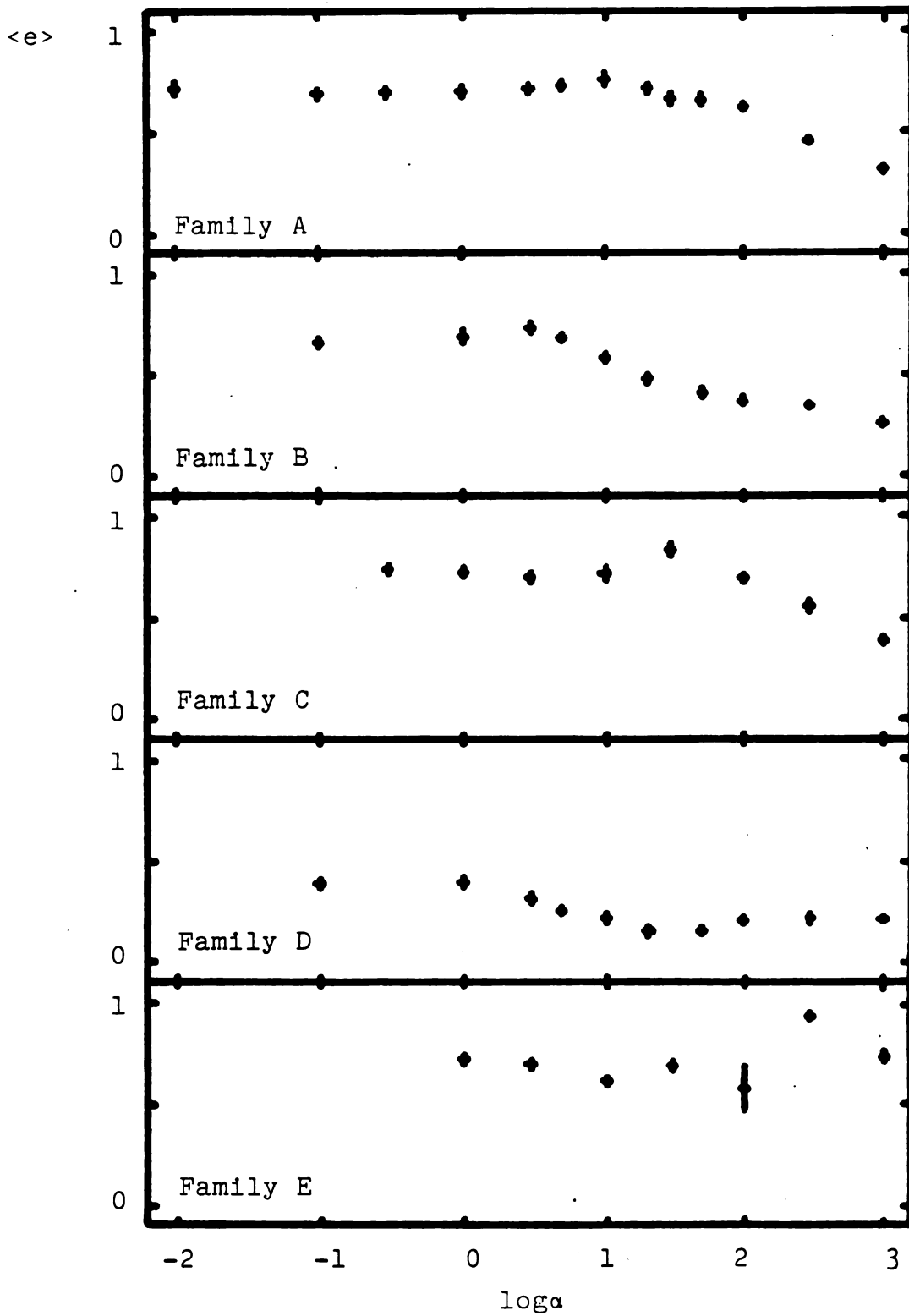


Figure 13. Average eccentricity versus $\log a$.

kinetic energy as the difference in the masses of the binary components increases. Thus, high-energy collisions can be very effective in disrupting one of the binaries. Figure 11 bears this out. As α increases for family E, the probability that only a single binary will remain increases. We have been able to offer support to Hills's postulate, but we see no way of ascertaining whether a given binary was formed through a single-binary or a binary-binary collision. We can say only that if the eccentricity of a binary is less than approximately 0.2, the probability is high that the binary has not undergone a collision of some type.

4.5. The Distance of Closest Approach

Although the collisions we have performed neglect the physical sizes of the stars, it is quite possible that a dynamical collision may precipitate a physical collision between stars in the system. If this occurs, then the assumptions implicit in this experiment no longer apply. (This experiment does not allow us to begin with four stars and end with three!) We can, however, obtain the likelihood that a physical collision occurred by examining the distance of closest approach between any two stars in the system.

Figure 14 summarizes the dependence of the logarithm of the average distance of closest approach on $\log \alpha$ and on the masses of the binary components. The vertical axis is the logarithm of the minimum distance of closest approach in units of the initial semi-major axis of the binary

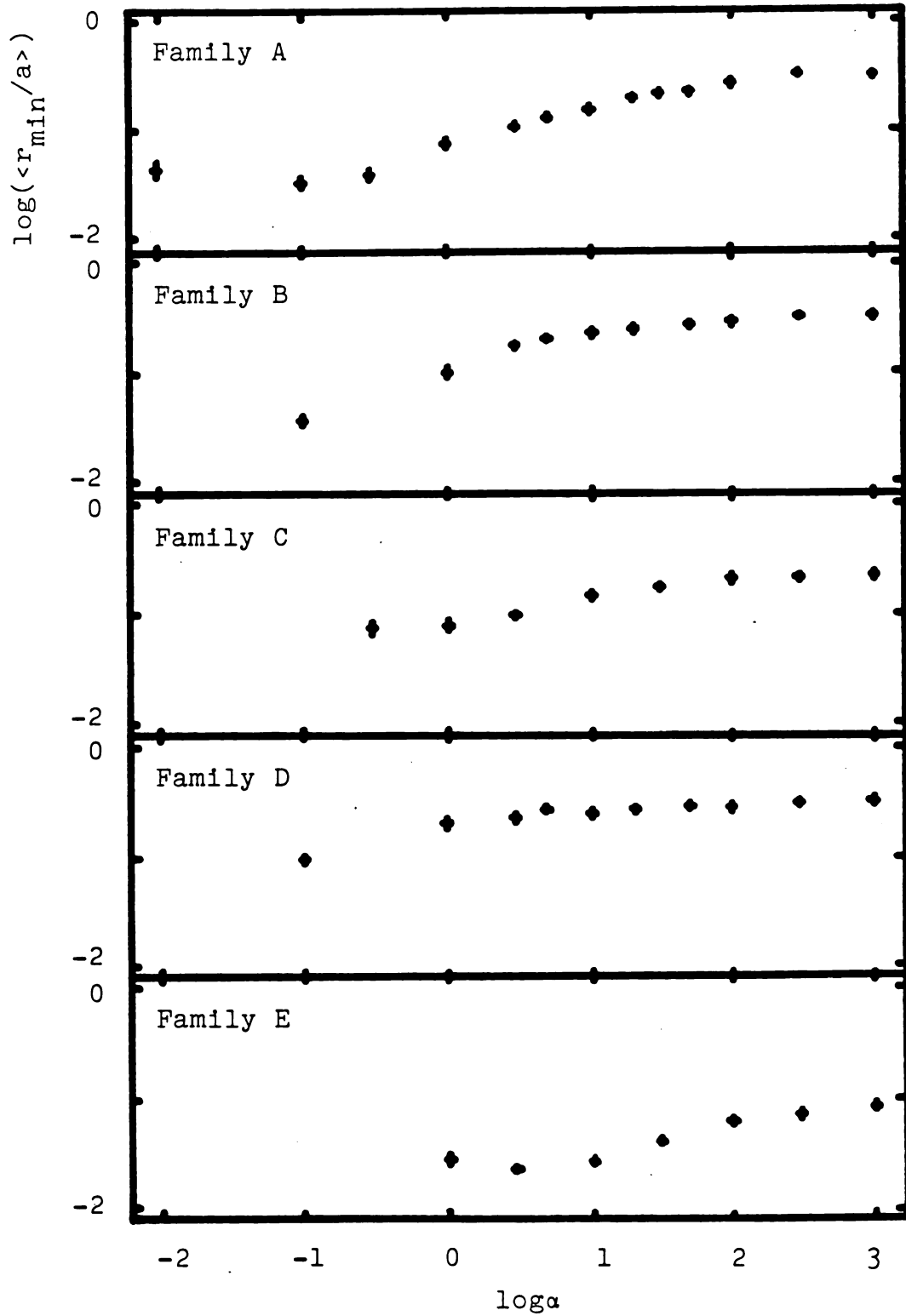


Figure 14. Logarithm of the average distance of closest approach versus $\log \alpha$.

containing m_1 and m_2 . As expected, this distance decreases with decreasing α . The unexpected occurrence is with family E; the distance of closest approach is between 0.210 and 0.085 for all α considered.

While we cannot predict actual physical collision rates without a knowledge of the stars composing the binaries or of the orbital elements of the binaries themselves, we can find the likelihood of physical collisions in a typical situation such as in dense, globular cluster cores. We will assume that the core contains equal mass binaries, each with components having mass $m=0.4M$, where M is the mass of the Sun. This gives a diameter for each star of $d=0.5D$, where D is the diameter of the Sun (Hills and Day 1976). Spitzer and Mathieu (1980) find from their computer models of globular clusters that the maximum α is about 0.03. A reasonable average α is then $\langle\alpha\rangle=0.1$, which we will assume. We will also assume $\langle v^2 \rangle^{1/2}=10$ km/s as obtained by Hills and Day (1976). These values give a semi-major axis for the orbit of a binary of $a=0.357$ A.U. resulting in $d/a=0.013$. From our experiment, the median of r_{\min}/a is 0.016 when $\alpha=0.1$. Thus we may conclude that binary collisions can significantly increase the rate of physical collisions between stars in globular cluster cores. The data indicate that, for every 100 binary-binary collisions, 40-50 of them may involve physical collisions. It seems that globular cluster cores can no longer be treated as a group of point masses; the physical sizes of the stars must be included so that the

effects of physical collisions and the possible coalescence of stars as well as very close approaches resulting in significant tidal distortion can be included in the models. Otherwise, an accurate picture of the dynamics of globular clusters will not be obtained.

CHAPTER 5
CONCLUSIONS

5.1. Comparison of Present with Previous Results

As mentioned in the Introduction, computer experiments have been performed for collisions between binary and single stars (Hills 1975; Hills and Fullerton 1980; Fullerton and Hills 1982). Therefore, it would be most instructive to compare our results with these previous results. Rather than compare all of our results, we will compare only those which can be associated quantitatively: namely, the energy exchanged by a collision and the relevant cross-section.

Before we can make comparisons between our data and the only comparable previously acquired data, that of Hills (1975) and Hills and Fullerton (1980), we must find conversion factors between their data and our data. (The experiments of Hills and Fullerton will be referred to collectively as HF.) HF's energies were measured as multiples of the total initial binding energy as are our's, except they had only a single binary where we have two. We would like to convert our energies into energies measured in terms of the binding energy of only one of the binaries. The relation which accomplishes this is

$$\xi' = (1+f_1/f_2)\xi. \quad (5.1)$$

f_2 is the fraction of the initial binding energy in the binary now considered to contain the reference energy and f_1 is the fraction in the other binary. The quantity in parentheses is the factor by which we must multiply the energy given in column five of the table in Appendix A to convert it to HF's units. These factors are given in Table

Table 4. Conversion factors from the present experiment to HF's experiment.

Present	HF	$1+f_1/f_2$	$(\xi'/\xi_{HF})_{\alpha=0}$
(1-1)-(1-1)	(1-1)-1	2	2.7
(3-3)-(1-1)	(3-3)-1	1.11	4.7
	(1-1)-3	10	3.7
(1-3)-(1-3)	(1-3)-1	2	5.5
	(1-3)-3	2	
(10-10)-(1-1)	(10-10)-1	1.01	253
	(1-1)-10	101	748
(1-10)-(1-10)	(1-10)-1	2	
	(1-10)-10	2	

4. The first column gives the family in the present experiment in terms of the masses while the second gives the

masses of families in HF's experiments. The third column gives the conversion factors described by equation (5.1). Into the last column of Table 4, we have entered the ratio of our exchanged energy in HF's units to HF's when $\alpha=0$. We used equation (4.8) to find the appropriate ξ 's for this experiment. $\alpha=0$ was chosen because, if $\alpha \neq 0$, α also must be transformed into HF's units. Direct comparison then becomes difficult because of the sparseness of data in both experiments. Blanks in Table 4 occur where data is not available for the single-binary collisions. While there appears to be no rule for finding ξ' given ξ_{HF} , we may conclude, not surprisingly, that a binary-binary collision releases several times the energy of a single-binary collision. The ratio $(\xi'/\xi_{HF})_{\alpha=0}$ increases rapidly with the largest mass star partaking in the collision.

It is difficult to compare the cross-sections obtained in the present experiment with those obtained by HF for the reason mentioned above, namely, α is different for the two experiments. Rather than attempt a conversion of α , we note that each of the curves in Figure 8 reaches a peak in the region $\alpha > \alpha_0$ as do the corresponding curves in Hills's (1975) Figure 8. As a comparison of the cross-section of the two experiments, we will compare the height of these peaks after applying equation (5.1) to the peak height of the present experiment. Hills's results will allow us to compare only the top three entries in Table 4. We find that the (1-1)-(1-1) case has a cross-section which is approximately

2.0 times the (1-1)-1 case. (3-3)-(1-1) versus (3-3)-1 gives a factor of 1.8 while (3-3)-(1-1) versus (1-1)-3 gives 16, both larger in the present experiments.

There are two reasons for the difference in the cross-sections of the binary-binary experiments compared with that of the single-binary, aside from simply a difference in the collision type. The binary-binary collisions have geometrical cross-sections that are a factor of four larger than the single-binary case. This is because there are two finite-sized binaries rather than a binary and a point mass. The second is the reason for the application of equation (5.1) to adjust the units of σ_E . Of course, these two explanations do not account for all of the differences in the two experiments. They do, however, help one to live with the large differences in the released energy obtained above.

5.2. Future Investigations of Binary-Binary Collisions

By performing this experiment and analyzing the subsequent data, we have begun to obtain an understanding of these collisions. However, the large majority of our collisions were soft collisions ($\xi < 0$). While these collisions can be quite well understood after this experiment, hard collisions are not well understood. This is because hard collisions can cost 100 times more than soft collisions. In addition, even with reduction, only about half of the hard collisions formed stable configurations within 10^5 integration steps. Because of this, our

conclusions for these collisions may be unreliable. Therefore, we need to simulate more hard collisions, allowing perhaps 10^6 integration steps. This would require a significant amount of computer time.

All collisions in this experiment were begun with the initial eccentricities of the binaries set to zero. While probably not a bad assumption if the binaries are undergoing their first collision, for subsequent collisions, the orbits are likely to be eccentric. We should investigate the effect of eccentricity of the binaries on the collisions.

We might, at some later time, wish to perform binary-binary collisions with differing values of β . The β 's used in this experiment were chosen so that the binaries had equal initial separations. While varying β might be interesting, when one binary is close, the collision results should be similar to those obtained in single-binary collisions. This should be verified, however.

The five families investigated provide us with a reasonable mass spectrum. Families B and D appear to describe the case of a massive binary colliding with a light binary quite well. Families C and E, however, which involve collisions between two binaries, each with components with quite different masses, do not appear to give a complete picture of this type of collision. We cannot state, with any degree of certainty, what will happen as the masses of the components become more discrepant. This also remains to be investigated.

The above "list of things to do" simply expresses the fact that there is a large parameter space to be investigated. While the completion of this investigation as described is important and necessary and should be carried out, a more expedient approach might be considered. Since one of the major uses of the results of this experiment was to be its application to clusters, we might consider modeling such clusters directly. The technique of reduction developed expressly for this experiment is ideally suited to such modeling. Not only would binary-binary collisions be considered, but higher order effects such as single-binary-binary and binary-binary-binary collisions would be automatically taken into account by the model. This might actually be the best next step, considering the expense of obtaining an understanding of the effects of binaries on real physical systems by the present technique. We have only begun to understand the effects of collisions between two binary systems on the evolution of a stellar system.

LIST OF REFERENCES

LIST OF REFERENCES

- Aarseth, S.J. and Hills, J.G. (1972) *Astronomy and Astrophysics* 21, 255, The Dynamical Evolution of a Stellar Cluster with Initial Subclustering.
- Bate, R.R, Mueller, D.D., and White, J.E. (1971) "Fundamentals of Astrodynamics", (New York: Dover Publications, Inc.).
- Bevington, P.R. (1969) "Data Reduction and Error Analysis for the Physical Sciences", (New York: McGraw-Hill Book Company).
- Fullerton, L.W. and Hills, J.G. (1982) *Astronomical Journal* 87, 175, Computer Simulations of Close Encounters Between Binary and Single Stars: The Effect of the Impact Velocity and the Stellar Masses.
- Heggie, D.C. (1972) A Multi-Particle Regularisation Technique. "Gravitational N-Body Problem" pp. 148-152. Ed. M. Lecar. (Dordrecht-Holland: D. Reidel Publishing Company).
- Heggie, D.C. (1975) *Monthly Notices of the Royal Astronomical Society* 173, 729, Binary Evolution in Stellar Dynamics.
- Hildebrand, F.B. (1974) "Introduction to Numerical Analysis", (New York: McGraw-Hill Book Company).
- Hills, J.G. (1975) *Astronomical Journal* 80, 809, Encounters Between Binary and Single Stars and Their Effect on the Dynamical Evolution of Stellar Systems.
- Hills, J.G. and Day, C.A. (1976) *Astrophysical Letters* 17, 87, Stellar Collisions in Globular Clusters.
- Hills, J.G. (1977) *Astronomical Journal* 82, 626, Exchange Collisions Between Binary and Single Stars.
- Hills, J.G. and Fullerton, L.W. (1980) *Astronomical Journal* 85, 1281, Computer Simulations of Close Encounters Between Single Stars and Hard Binaries.

- Hoffer, J.B. (1982) *Celestial Mechanics*, submitted, A Technique for the Computer Simulation of the Dynamics of Stellar Systems Containing Tightly-Bound Binary Star Systems.
- Larson, R.B. (1981) *Monthly Notices of the Royal Astronomical Society* 194, 809, Turbulence and Star Formation in Molecular Clouds.
- Marion J.B. (1970) "Classical Dynamics of Particles and Systems" (Second Edition), (New York: Academic Press).
- Moulton F.R. (1914) "An Introduction to Celestial Mechanics" (Second Edition), (New York: The MacMillan Company).
- Saslaw, W.C., Valtonen, M.J., and Aarseth, S.J. (1974) *Astrophysical Journal* 190, 253, The Gravitational Slingshot and the Structure of Extragalactic Radio Sources.
- Spitzer, L. and Mathieu, R.D. (1980) *Astrophysical Journal* 241, 618, Random Gravitational Encounters and the Evolution of Spherical Systems. VIII. Clusters with an Initial Distribution of Binaries.
- Valtonen, M.J. (1975) *Memoirs of the Royal Astronomical Society* 80, 77, Statistics of Three-Body Experiments: Probability of Escape and Capture.

APPENDICES

APPENDIX A

THE DATA

The following table is a summary of all the data regarding collisions between two binary stars used in compiling the conclusions of this dissertation. All of the entries should be self-explanatory for anyone who has read the text of this dissertation. A quantity listed immediately after a +- is the absolute error of the preceding entry.

Table 5. A summary of the results of the collisions.

Num	α	β	p	ξ	$\langle e \rangle$	$\langle r_{min}/a \rangle$	PNC	PE	PSB	PD	Runs
FAMILY A: (1-1)-(1-1)											
1	.10	.01	.00	-.011+-0.000	.002+-0.001	.441+-0.029	.000	.000	1.000	.000	98
2	.01	1.00	.00	.830+-0.180	.720+-0.029	.044+-0.009	.097	.258	.645	.000	31
3	.10	1.00	.00	.716+-0.057	.692+-0.018	.033+-0.004	.019	.157	.824	.000	159
4	.30	1.00	.00	.283+-0.041	.694+-0.019	.039+-0.004	.040	.167	.794	.000	126
5	1.01	1.00	.00	-.123+-0.072	.693+-0.025	.075+-0.007	.090	.154	.769	.000	78
6	1.01	1.00	1.00	-.229+-0.035	.696+-0.018	.092+-0.007	.064	.115	.827	.000	156
7	1.01	1.00	2.00	-.177+-0.029	.633+-0.015	.215+-0.013	.553	.047	.406	.000	170
8	1.01	1.00	3.00	-.060+-0.017	.355+-0.014	.530+-0.019	.811	.024	.171	.000	164
9	1.01	1.00	4.00	-.004+-0.006	.204+-0.009	.712+-0.011	1.000	.000	.000	.000	200
10	1.01	1.00	5.00	.008+-0.001	.082+-0.003	.871+-0.005	1.000	.000	.000	.000	200
11	1.01	1.00	6.00	.001+-0.000	.030+-0.001	.953+-0.002	1.000	.000	.000	.000	200
12	1.01	1.00	7.00	.000+-0.000	.011+-0.000	.982+-0.001	1.000	.000	.000	.000	200
13	3.00	1.00	.00	-.488+-0.037	.706+-0.019	.108+-0.006	.005	.053	.747	.200	190
14	3.00	1.00	.50	-.611+-0.024	.759+-0.016	.135+-0.007	.045	.005	.783	.172	198
15	3.00	1.00	1.00	-.443+-0.029	.644+-0.018	.190+-0.010	.242	.020	.616	.121	198
16	3.00	1.00	1.50	-.219+-0.028	.528+-0.013	.385+-0.013	.650	.005	.260	.085	200
17	3.00	1.00	2.00	-.142+-0.021	.348+-0.011	.625+-0.014	.805	.000	.180	.015	200

Table 5 (cont'd.).

Num	α	β	p	ξ	$\langle e \rangle$	$\langle r_{min}/a \rangle$	PNC	PE	PSB	PD	Runs
18	3.00	1.00	3.00	-.019+-007	.161+-006	.802+-009	1.000	.000	.000	.000	200
19	3.00	1.00	4.00	.002+-002	.072+-003	.894+-005	1.000	.000	.000	.000	200
20	3.00	1.00	5.00	.001+-001	.035+-001	.947+-002	1.000	.000	.000	.000	200
21	5.00	1.00	.00	-.467+-043	.724+-020	.132+-000	.010	.036	.490	.469	196
22	5.00	1.00	.25	-.526+-031	.746+-021	.137+-007	.051	.005	.497	.446	195
23	5.00	1.00	.50	-.480+-032	.695+-019	.175+-008	.135	.005	.480	.380	200
24	5.00	1.00	1.00	-.266+-032	.581+-016	.256+-011	.465	.000	.305	.230	200
25	5.00	1.00	1.50	-.137+-024	.414+-012	.492+-013	.775	.000	.175	.050	200
26	5.00	1.00	2.00	-.081+-016	.263+-009	.700+-012	.930	.000	.070	.000	200
27	5.00	1.00	2.50	-.027+-009	.174+-006	.787+-010	1.000	.000	.000	.000	200
28	5.00	1.00	3.00	-.007+-005	.114+-004	.844+-007	1.000	.000	.000	.000	200
29	5.00	1.00	3.50	-.000+-003	.079+-003	.885+-005	1.000	.000	.000	.000	200
30	5.00	1.00	4.00	.001+-002	.056+-002	.916+-004	1.000	.000	.000	.000	200
31	5.00	1.00	6.00	.000+-000	.015+-001	.978+-001	1.000	.000	.000	.000	200
32	10.00	1.00	.00	-.497+-055	.759+-024	.152+-008	.025	.005	.380	.590	200
33	10.00	1.00	.13	-.540+-030	.754+-022	.152+-008	.025	.000	.445	.530	200
34	10.00	1.00	.25	-.536+-027	.753+-018	.162+-007	.090	.000	.500	.410	200
35	10.00	1.00	.50	-.489+-024	.631+-018	.216+-008	.185	.000	.570	.245	200
36	10.00	1.00	1.00	-.227+-028	.519+-014	.347+-013	.645	.000	.265	.090	200
37	10.00	1.00	1.50	-.095+-018	.314+-010	.633+-013	.945	.000	.050	.005	200
38	10.00	1.00	2.00	-.034+-010	.179+-006	.791+-010	1.000	.000	.000	.000	200
39	10.00	1.00	2.50	-.014+-006	.111+-003	.857+-007	1.000	.000	.000	.000	200

Table 5 (cont'd.).

Num	α	β	p	ξ	$\langle e \rangle$	$\langle r_{min}/a \rangle$	PNC	PE	PSB	PD	Runs
40	20.00	1.00	.00	-.567+-0.027	.719+-0.022	.198+-0.010	.070	.005	.435	.490	200
41	20.00	1.00	.25	-.469+-0.028	.688+-0.019	.186+-0.009	.188	.005	.472	.335	197
42	20.00	1.00	.50	-.318+-0.026	.581+-0.016	.244+-0.009	.490	.000	.360	.150	200
43	20.00	1.00	1.00	-.120+-0.022	.408+-0.013	.453+-0.014	.825	.000	.130	.045	200
44	20.00	1.00	1.50	-.035+-0.011	.214+-0.007	.726+-0.011	1.000	.000	.000	.000	200
45	20.00	1.00	2.00	-.010+-0.006	.118+-0.003	.842+-0.008	1.000	.000	.000	.000	200
46	30.00	1.00	.00	-.444+-0.026	.660+-0.020	.213+-0.010	.205	.000	.390	.405	200
47	30.00	1.00	.06	-.452+-0.026	.650+-0.024	.197+-0.010	.167	.000	.434	.399	198
48	30.00	1.00	.13	-.442+-0.025	.653+-0.020	.196+-0.010	.185	.000	.425	.390	200
49	30.00	1.00	.25	-.443+-0.026	.648+-0.017	.212+-0.009	.315	.000	.490	.195	200
50	30.00	1.00	.50	-.297+-0.022	.523+-0.014	.265+-0.009	.581	.000	.313	.111	198
51	30.00	1.00	.75	-.163+-0.023	.450+-0.013	.344+-0.013	.745	.000	.135	.120	200
52	30.00	1.00	1.00	-.100+-0.019	.359+-0.012	.495+-0.014	.895	.000	.080	.025	200
53	30.00	1.00	1.50	-.021+-0.008	.164+-0.005	.773+-0.009	1.000	.000	.000	.000	200
54	30.00	1.00	2.00	-.007+-0.004	.090+-0.002	.877+-0.006	1.000	.000	.000	.000	200
55	30.00	1.00	2.50	-.003+-0.003	.057+-0.002	.917+-0.004	1.000	.000	.000	.000	200
56	30.00	1.00	3.00	-.002+-0.002	.039+-0.001	.942+-0.003	1.000	.000	.000	.000	200
57	30.00	1.00	3.50	-.001+-0.001	.029+-0.001	.957+-0.002	1.000	.000	.000	.000	200
58	30.00	1.00	4.00	-.001+-0.001	.022+-0.001	.967+-0.002	1.000	.000	.000	.000	200
59	30.00	1.00	4.50	-.000+-0.001	.017+-0.000	.974+-0.001	1.000	.000	.000	.000	200
60	50.00	1.00	.00	-.424+-0.028	.654+-0.017	.226+-0.009	.290	.000	.455	.255	200
61	50.00	1.00	.50	-.222+-0.022	.477+-0.013	.283+-0.009	.675	.000	.245	.080	200

Table 5 (cont'd.).

Num	α	β	p	ξ	$\langle e \rangle$	$\langle r_{min}/a \rangle$	PNC	PE	PSB	PD	Runs
62	100.00	1.00	.00	-.285+-0.026	.622+-0.013	.267+-0.010	.565	.000	.260	.175	200
63	100.00	1.00	.10	-.328+-0.027	.613+-0.012	.246+-0.099	.590	.000	.290	.120	200
64	100.00	1.00	.20	-.288+-0.024	.549+-0.012	.248+-0.009	.710	.000	.215	.075	200
65	100.00	1.00	.30	-.204+-0.021	.477+-0.012	.261+-0.008	.800	.000	.140	.060	200
66	100.00	1.00	.40	-.176+-0.020	.429+-0.013	.286+-0.009	.810	.000	.160	.030	200
67	100.00	1.00	.50	-.131+-0.018	.371+-0.012	.315+-0.010	.825	.000	.120	.055	200
68	100.00	1.00	.75	-.079+-0.017	.303+-0.012	.418+-0.012	.940	.000	.045	.015	200
69	100.00	1.00	1.00	-.043+-0.011	.212+-0.010	.584+-0.014	.985	.000	.015	.000	200
70	100.00	1.00	1.50	-.009+-0.004	.088+-0.002	.854+-0.007	1.000	.000	.000	.000	200
71	300.00	1.00	.00	-.157+-0.015	.448+-0.009	.322+-0.008	.838	.000	.110	.072	400
72	300.00	1.00	.10	-.150+-0.021	.421+-0.012	.294+-0.010	.875	.000	.105	.020	200
73	300.00	1.00	.20	-.104+-0.016	.371+-0.009	.271+-0.009	.935	.000	.035	.030	200
74	300.00	1.00	.30	-.109+-0.015	.340+-0.011	.269+-0.008	.930	.000	.065	.005	200
75	300.00	1.00	.40	-.112+-0.017	.301+-0.012	.285+-0.008	.940	.000	.050	.010	200
76	300.00	1.00	.50	-.082+-0.016	.265+-0.012	.310+-0.009	.920	.000	.060	.020	200
77	300.00	1.00	.60	-.049+-0.012	.235+-0.010	.342+-0.010	.955	.000	.030	.015	200
78	300.00	1.00	.70	-.030+-0.010	.210+-0.010	.389+-0.012	.970	.000	.015	.015	200
79	300.00	1.00	.80	-.041+-0.012	.189+-0.011	.449+-0.013	.970	.000	.030	.000	200
80	300.00	1.00	.90	-.028+-0.010	.155+-0.009	.521+-0.014	.980	.000	.015	.005	200
81	300.00	1.00	1.00	-.018+-0.008	.124+-0.006	.600+-0.014	.995	.000	.005	.000	200
82	300.00	1.00	1.10	-.010+-0.008	.098+-0.004	.676+-0.013	1.000	.000	.000	.000	200
83	300.00	1.00	1.20	-.006+-0.004	.080+-0.002	.747+-0.012	1.000	.000	.000	.000	200
84	300.00	1.00	1.30	-.004+-0.003	.067+-0.002	.810+-0.010	1.000	.000	.000	.000	200

Table 5 (cont'd.).

Num	α	β	p	ξ	$\langle e \rangle$	$\langle r_{\min}/a \rangle$	PNC	PE	PSB	PD	Runs
85	300.00	1.00	1.40	-.003+-003	.058+-001	.859+-008	1.000	.000	.000	.000	200
86	300.00	1.00	1.50	-.002+-002	.050+-001	.893+-006	1.000	.000	.000	.000	200
87	300.00	1.00	1.60	-.001+-002	.044+-001	.918+-004	1.000	.000	.000	.000	200
88	300.00	1.00	1.70	-.001+-002	.039+-001	.936+-003	1.000	.000	.000	.000	200
89	1000.00	1.00	.00	-.083+-018	.311+-014	.319+-011	.925	.000	.055	.020	200
90	1000.00	1.00	.10	-.070+-015	.273+-011	.289+-011	.955	.000	.040	.005	200
91	1000.00	1.00	.20	-.055+-012	.239+-009	.261+-009	.980	.000	.010	.010	200
92	1000.00	1.00	.30	-.049+-013	.205+-010	.260+-008	.955	.000	.040	.005	200
93	1000.00	1.00	.40	-.036+-010	.180+-009	.278+-008	.980	.000	.020	.000	200
94	1000.00	1.00	.50	-.030+-009	.164+-010	.310+-009	.990	.000	.010	.000	200
95	1000.00	1.00	.60	-.035+-009	.145+-009	.345+-010	.985	.000	.015	.000	200
96	1000.00	1.00	.70	-.027+-008	.126+-008	.391+-011	.995	.000	.005	.000	200
97	1000.00	1.00	.80	-.018+-007	.102+-006	.451+-013	.995	.000	.000	.005	200
98	1000.00	1.00	.90	-.012+-005	.083+-005	.523+-014	.985	.000	.010	.005	200
99	1000.00	1.00	1.00	-.005+-003	.065+-003	.602+-014	1.000	.000	.000	.000	200
100	1000.00	1.00	1.10	-.003+-003	.052+-002	.683+-014	1.000	.000	.000	.000	200
101	1000.00	1.00	1.20	-.002+-002	.043+-001	.758+-013	1.000	.000	.000	.000	200
102	1000.00	1.00	1.30	-.001+-002	.036+-001	.624+-011	1.000	.000	.000	.000	200
103	1000.00	1.00	1.40	-.001+-001	.031+-001	.878+-009	1.000	.000	.000	.000	200
104	1000.00	1.00	1.50	-.001+-001	.027+-001	.917+-007	1.000	.000	.000	.000	200

Table 5 (cont'd.).

Num	α	β	p	ξ	$\langle e \rangle$	$\langle r_{min}/a \rangle$	PNC	PE	PSB	PD	Runs
FAMILY B: (3-3)-(1-1)											
1	.10	.11	.00	.491+-0.048	.660+-0.019	.037+-0.003	.009	.054	.946	.000	112
2	1.01	.11	.00	-.238+-0.071	.687+-0.028	.100+-0.012	.037	.148	.815	.000	54
3	3.00	.11	.00	-.412+-0.040	.727+-0.015	.176+-0.009	.030	.005	.730	.235	200
4	3.00	.11	1.00	-.128+-0.027	.479+-0.015	.292+-0.012	.335	.000	.600	.065	200
5	3.00	.11	2.00	-.046+-0.009	.256+-0.009	.701+-0.017	.820	.000	.180	.000	200
6	3.00	.11	3.00	-.006+-0.003	.148+-0.006	.809+-0.011	.995	.000	.005	.000	200
7	3.00	.11	4.00	-.000+-0.001	.076+-0.003	.879+-0.007	1.000	.000	.000	.000	200
8	5.00	.11	.00	-.316+-0.039	.679+-0.017	.202+-0.009	.025	.005	.685	.285	200
9	5.00	.11	1.00	-.099+-0.023	.410+-0.013	.342+-0.013	.410	.000	.555	.035	200
10	5.00	.11	2.00	-.024+-0.006	.219+-0.008	.746+-0.015	.920	.000	.080	.000	200
11	5.00	.11	3.00	-.004+-0.002	.108+-0.004	.861+-0.009	1.000	.000	.000	.000	200
12	5.00	.11	4.00	-.001+-0.001	.058+-0.002	.915+-0.006	1.000	.000	.000	.000	200
13	10.00	.11	.00	-.233+-0.032	.581+-0.015	.224+-0.010	.045	.000	.750	.205	200
14	10.00	.11	1.00	-.062+-0.018	.353+-0.012	.405+-0.015	.580	.000	.410	.010	200
15	10.00	.11	2.00	-.010+-0.004	.167+-0.006	.806+-0.012	1.000	.000	.000	.000	200
16	10.00	.11	3.00	-.002+-0.002	.073+-0.002	.897+-0.007	1.000	.000	.000	.000	200
17	10.00	.11	4.00	-.001+-0.001	.040+-0.001	.939+-0.004	1.000	.000	.000	.000	200

Table 5 (cont'd.).

Num	α	β	p	ξ	$\langle e \rangle$	$\langle r_{min}/a \rangle$	PNC	PE	PSB	PD	Runs
18	20.00	.11	.00	-.212+-0.025	.479+-0.016	.248+-0.011	.130	.000	.710	.160	200
19	20.00	.11	1.00	-.055+-0.012	.311+-0.012	.484+-0.016	.770	.000	.230	.000	200
20	20.00	.11	2.00	-.007+-0.003	.114+-0.004	.851+-0.010	1.000	.000	.000	.000	200
21	20.00	.11	3.00	-.002+-0.001	.050+-0.001	.926+-0.005	1.000	.000	.000	.000	200
22	20.00	.11	4.00	-.001+-0.001	.028+-0.001	.956+-0.003	1.000	.000	.000	.000	200
23	50.00	.11	.00	-.121+-0.022	.407+-0.015	.269+-0.010	.250	.000	.685	.065	200
24	50.00	.11	.50	-.063+-0.014	.328+-0.013	.295+-0.009	.600	.000	.380	.020	200
25	50.00	.11	1.00	-.017+-0.008	.251+-0.010	.521+-0.014	.910	.000	.090	.000	200
26	50.00	.11	2.00	-.002+-0.002	.069+-0.002	.900+-0.006	1.000	.000	.000	.000	200
27	50.00	.11	3.00	-.001+-0.001	.030+-0.001	.951+-0.003	1.000	.000	.000	.000	200
28	50.00	.11	4.00	-.000+-0.000	.017+-0.000	.971+-0.002	1.000	.000	.000	.000	200
29	100.00	.11	.00	-.119+-0.013	.363+-0.010	.285+-0.008	.408	.000	.550	.043	400
30	100.00	.11	.20	-.071+-0.014	.317+-0.013	.236+-0.009	.405	.000	.585	.010	200
31	100.00	.11	.40	-.076+-0.012	.302+-0.013	.272+-0.009	.575	.000	.410	.015	200
32	100.00	.11	.60	-.049+-0.010	.299+-0.010	.296+-0.010	.665	.000	.330	.005	200
33	100.00	.11	.80	-.035+-0.013	.308+-0.011	.349+-0.013	.780	.000	.220	.000	200
34	100.00	.11	1.00	-.008+-0.008	.229+-0.009	.481+-0.014	.915	.000	.085	.000	200
35	100.00	.11	1.20	-.006+-0.003	.132+-0.005	.709+-0.013	.995	.000	.005	.000	200
36	100.00	.11	1.40	-.003+-0.002	.096+-0.003	.813+-0.010	1.000	.000	.000	.000	200
37	100.00	.11	1.60	-.002+-0.002	.073+-0.002	.878+-0.007	1.000	.000	.000	.000	200
38	100.00	.11	1.80	-.001+-0.001	.057+-0.002	.911+-0.006	1.000	.000	.000	.000	200
39	100.00	.11	2.00	-.001+-0.001	.046+-0.001	.928+-0.005	1.000	.000	.000	.000	200

Table 5 (cont'd.).

Num	α	β	p	ξ	$\langle e \rangle$	$\langle r_{\min}/a \rangle$	PNC	PE	PSB	PD	Runs
40	100.00	.11	2.20	-.001+-001	.038+-001	.939+-004	1.000	.000	.000	.000	200
41	100.00	.11	2.40	-.001+-001	.032+-001	.948+-003	1.000	.000	.000	.000	200
42	100.00	.11	2.60	-.000+-001	.027+-001	.955+-003	1.000	.000	.000	.000	200
43	100.00	.11	2.80	-.000+-001	.024+-001	.961+-003	1.000	.000	.000	.000	200
44	100.00	.11	3.00	-.000+-001	.020+-001	.966+-002	1.000	.000	.000	.000	200
45	300.00	.11	.00	-.053+-010	.342+-008	.323+-008	.740	.000	.238	.023	400
46	300.00	.11	.20	-.015+-010	.299+-010	.252+-009	.795	.000	.190	.015	200
47	300.00	.11	.40	-.023+-008	.250+-009	.284+-008	.900	.000	.095	.005	200
48	300.00	.11	.60	-.017+-007	.208+-009	.332+-011	.905	.000	.085	.010	200
49	300.00	.11	.80	-.015+-006	.174+-008	.439+-014	.960	.000	.040	.000	200
50	300.00	.11	1.00	-.008+-005	.123+-006	.590+-014	.995	.000	.005	.000	200
51	300.00	.11	1.20	-.002+-002	.080+-003	.735+-012	1.000	.000	.000	.000	200
52	300.00	.11	1.40	-.001+-001	.057+-002	.847+-009	1.000	.000	.000	.000	200
53	300.00	.11	1.60	-.001+-001	.043+-001	.914+-005	1.000	.000	.000	.000	200
54	300.00	.11	1.80	-.000+-001	.033+-001	.944+-004	1.000	.000	.000	.000	200
55	300.00	.11	2.00	-.000+-001	.027+-001	.955+-003	1.000	.000	.000	.000	200
56	1000.00	.11	.00	-.040+-012	.258+-010	.326+-012	.865	.000	.120	.015	200
57	1000.00	.11	.10	-.030+-007	.237+-007	.278+-010	.930	.000	.070	.000	200
58	1000.00	.11	.20	-.016+-007	.211+-008	.259+-009	.950	.000	.045	.005	200
59	1000.00	.11	.30	-.016+-005	.190+-007	.265+-008	.965	.000	.035	.000	200
60	1000.00	.11	.40	-.015+-007	.164+-008	.291+-008	.960	.000	.040	.000	200
61	1000.00	.11	.50	-.019+-007	.142+-008	.324+-009	.970	.000	.030	.000	200

Table 5 (cont'd.).

Num	α	β	p	ξ	$\langle e \rangle$	$\langle r_{min}/a \rangle$	PNC	PE	PSB	PD	Runs
62	1000.00	.11	.60	-.009+-0.004	.125+-0.006	.360+-0.009	.985	.000	.015	.000	200
63	1000.00	.11	.70	-.006+-0.003	.111+-0.005	.406+-0.011	.990	.000	.010	.000	200
64	1000.00	.11	.80	-.004+-0.003	.098+-0.005	.463+-0.012	1.000	.000	.000	.000	200
65	1000.00	.11	.90	-.002+-0.002	.080+-0.004	.530+-0.014	.995	.000	.000	.005	200
66	1000.00	.11	1.00	-.002+-0.002	.068+-0.004	.607+-0.014	1.000	.000	.000	.000	200
67	3.00	1.00	.00	-.391+-0.013	.423+-0.015	.059+-0.001	.576	.000	.409	.020	198
68	3.00	1.00	1.00	-.036+-0.012	.172+-0.007	.063+-0.001	.980	.000	.020	.000	200
69	3.00	1.00	2.00	-.002+-0.003	.036+-0.002	.064+-0.001	1.000	.000	.000	.000	200
70	3.00	1.00	3.00	-.000+-0.001	.015+-0.001	.065+-0.001	1.000	.000	.000	.000	200
71	3.00	1.00	4.00	-.000+-0.000	.007+-0.000	.065+-0.001	1.000	.000	.000	.000	200
72	5.00	1.00	.00	-.312+-0.014	.408+-0.012	.056+-0.001	.700	.000	.280	.020	200
73	5.00	1.00	1.00	-.015+-0.008	.128+-0.005	.059+-0.000	1.000	.000	.000	.000	200
74	5.00	1.00	2.00	-.000+-0.002	.028+-0.001	.056+-0.000	1.000	.000	.000	.000	200
75	5.00	1.00	3.00	-.000+-0.001	.012+-0.000	.057+-0.000	1.000	.000	.000	.000	200
76	10.00	1.00	.00	-.212+-0.016	.362+-0.010	.065+-0.001	.815	.000	.165	.020	200
77	10.00	1.00	1.00	-.003+-0.005	.082+-0.003	.067+-0.000	1.000	.000	.000	.000	200
78	10.00	1.00	2.00	.001+-0.001	.019+-0.001	.067+-0.000	1.000	.000	.000	.000	200
79	20.00	1.00	.00	-.152+-0.015	.305+-0.009	.063+-0.000	.890	.000	.095	.015	200
80	20.00	1.00	1.00	-.007+-0.004	.061+-0.002	.064+-0.000	1.000	.000	.000	.000	200
81	20.00	1.00	2.00	-.001+-0.001	.014+-0.000	.064+-0.000	1.000	.000	.000	.000	200

Table 5 (cont'd.).

Num	α	β	p	ξ	$\langle e \rangle$	$\langle r_{min}/a \rangle$	PNC	PE	PSB	PD	Runs
FAMILY C: (1-3)-(1-3)											
1	.30	1.00	.00	.476+-0.058	.738+-0.018	.074+-0.006	.019	.453	.528	.000	106
2	1.01	1.00	.00	-.154+-0.037	.722+-0.019	.075+-0.006	.000	.386	.614	.000	114
3	3.00	1.00	.00	-.393+-0.038	.689+-0.019	.097+-0.006	.000	.139	.619	.242	194
4	10.00	1.00	.00	-.525+-0.071	.715+-0.041	.146+-0.007	.000	.035	.105	.860	200
5	30.00	1.00	.00	-.707+-0.024	.841+-0.019	.173+-0.008	.035	.005	.354	.606	198
6	100.00	1.00	.00	-.435+-0.026	.689+-0.014	.207+-0.009	.337	.000	.397	.266	199
7	300.00	1.00	.00	-.277+-0.026	.551+-0.014	.214+-0.009	.620	.000	.255	.125	200
8	1000.00	1.00	.00	-.105+-0.020	.388+-0.014	.224+-0.009	.875	.000	.095	.030	200
FAMILY D: (10-10)-(1-1)											
1	.10	.01	.00	.136+-0.013	.387+-0.014	.092+-0.006	.000	.000	1.000	.000	152
2	1.01	.01	.00	-.125+-0.014	.385+-0.006	.194+-0.006	.000	.000	1.000	.000	393

Table 5 (cont'd.).

Num	α	β	p	ξ	$\langle e \rangle$	$\langle r_{min}/a \rangle$	PNC	PE	PSB	PD	Runs
3	3.00	.01	.00	-.094+-.020	.307+-.012	.223+-.009	.000	.000	.990	.010	200
4	5.00	.01	.00	-.077+-.016	.247+-.011	.257+-.010	.045	.000	.950	.005	200
5	10.00	.01	.00	-.026+-.014	.213+-.011	.241+-.010	.035	.000	.945	.020	200
6	20.00	.01	.00	-.030+-.010	.149+-.009	.268+-.010	.060	.000	.930	.010	200
7	50.00	.01	.00	-.018+-.008	.147+-.010	.282+-.011	.165	.000	.820	.015	200
8	100.00	.01	.00	-.005+-.005	.198+-.013	.279+-.010	.400	.000	.595	.005	200
9	300.00	.01	.00	-.008+-.003	.219+-.011	.302+-.011	.635	.000	.365	.000	200
10	1000.00	.01	.00	-.003+-.002	.210+-.008	.320+-.011	.845	.000	.155	.000	200
FAMILY E: (1-10)-(1-10)											
1	1.01	1.00	.00	-.359+-.049	.719+-.019	.028+-.002	.000	.330	.670	.000	94
2	3.00	1.00	.00	-.441+-.027	.693+-.013	.022+-.001	.000	.419	.470	.111	198
3	10.00	1.00	.00	-.303+-.033	.604+-.016	.026+-.001	.000	.410	.430	.160	200

Table 5 (cont'd.).

Num	α	β	p	ξ	$\langle e \rangle$	$\langle r_{min}/a \rangle$	PNC	PE	PSB	PD	Runs
4	30.00	1.00	.00	-.482+-0.039	.682+-0.026	.039+-0.002	.000	.090	.325	.585	200
5	100.00	1.00	.00	-.587+-0.112	.572+-0.111	.061+-0.003	.000	.005	.040	.955	200
6	300.00	1.00	.00	-.787+-0.027	.935+-0.014	.071+-0.003	.010	.000	.155	.835	200
7	1000.00	1.00	.00	-.449+-0.031	.737+-0.016	.084+-0.003	.210	.000	.375	.415	200

APPENDIX B

GLOSSARY OF TERMS

The following glossary contains the definitions of some of the terms used in this dissertation. The orbital elements are defined using Figures 15 and 16, which are also contained in Appendix B.

GLOSSARY OF TERMS

- α - the ratio of the kinetic energy of the binaries at infinite separation to the energy required to dissociate both binaries.
- anomaly, eccentric - (ψ) the angular position of a fictitious point related to the real position of the orbiting object, but measured in a coordinate system centered on the center of the orbital ellipse (see Figure 16).
- anomaly, mean - (M)= $2\pi t/\tau$ where t is the time since periastron passage and τ is the orbital period.
- anomaly, true - (θ) the angular position of the object in orbit relative to periastron (see Figures 15 and 16).
- ascending node - the point where the orbiting body crosses the reference ellipse from south to north.
- ascending node, longitude of - (Ω) the angle between a reference point and the point where the orbiting body crosses the reference ellipse from south to north (see Figure 15).
- β - the ratio of the binding energy of the second binary to the binding energy of the first binary.
- eccentricity - (e)= $(1-(b/a)^2)^{1/2}$ a measure of the shape of the orbital ellipse.
- inclination - (i) the angle between the orbital angular momentum and some reference direction (see Figure 15).
- periastron - the point of closest approach in the orbit.
- periastron passage, argument of - (ω) the angle between the ascending node and the point of closest approach in the orbit (see Figure 15).
- semi-major axis - (a) half the length of the line segment which passes through both foci of the orbital ellipse and terminates on the orbital ellipse (see Figure 15).
- semi-minor axis - (b) half the length of the line segment which bisects the line segment passing through both foci of the orbital ellipse and terminating on the orbital ellipse (see Figure 15).

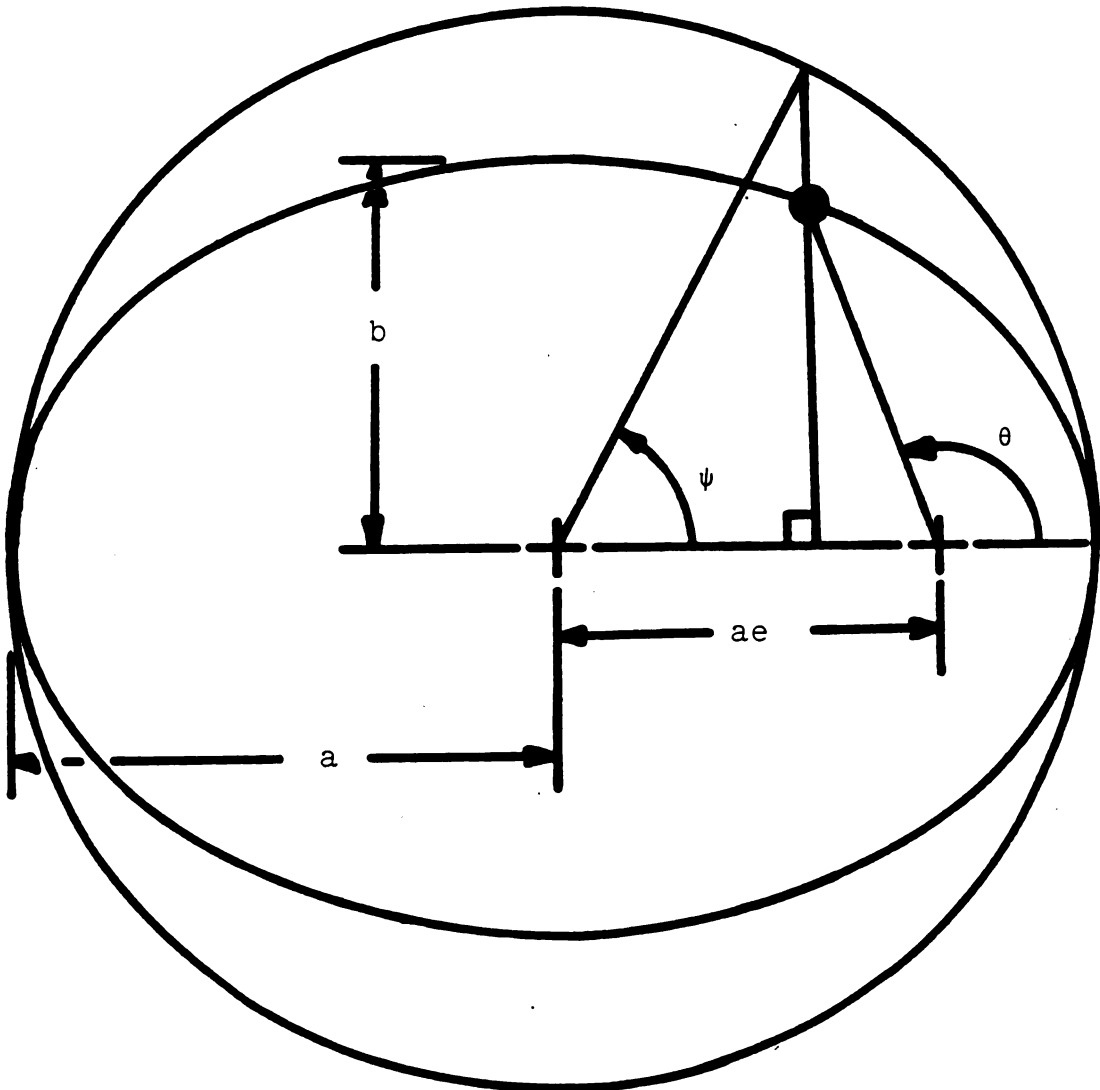


Figure 16. The orbital plane.